GCA-TR-70-11-N

N71-17052

NASA CR116441

INVESTIGATION OF THE D AND E REGIONS OF THE IONOSPHERE

L. G. Smith

CASE COPY FILE

Bedford, Massachusetts

FINAL REPORT

CONTRACT NO. NASW-1402

Prepared for
NATIONAL AERONAUTICS AND SPACE ADMINISTRATION
HEADQUARTERS
WASHINGTON, D. C.

January 1971

GCA-TR-70-11-N

INVESTIGATION OF THE D AND E REGIONS OF THE IONOSPHERE

L. G. Smith

GCA CORPORATION
GCA TECHNOLOGY DIVISION
Bedford, Massachusetts

FINAL REPORT

Contract No. NASW-1402

January 1971

Prepared for

NATIONAL AERONAUTICS AND SPACE ADMINISTRATION
Headquarters
Washington, D.C.

TABLE OF CONTENTS

Section	Title	Page
	SUMMARY	1
I	INTRODUCTION	1
II	EXPERIMENTAL PROGRAM	6
	A. General	6
	B. Nike Apache 14.270	6
	C. Nike Apaches 14.271 and 14.272	7
	D. Nike Apaches 14.274, 14.302, 14.304 and 14.303	8
	E. Nike Apache 14.275	12
	F. Nike Apache 14.273	14
	G. Nike Apaches 14.305, 14.308 and 14.309	15
	H. Nike Apaches 14.358, 14.359, 14.360 and 14.361	16
	I. Nike Apaches 14.391 and 14.392	18
	J. Nike Apache 14.393	19
	K. Nike Apache 14.395	22
	L. Nike Apache 14.394	22
	M. Vehicle Performance	23
III	INSTRUMENTATION	25
	A. General	25
	B. Type A Payloads	28
	C. Type B payloads	34
	D. Type C Payload	34
IV	ELECTRON TEMPERATURE PROBE	54
	A. Principle of Operation	54
	B. Instrument Operation	63
	C. Circuit Details	64
	D. Performance	73
	REFERENCES	77

INVESTIGATION OF THE D AND E REGIONS OF THE IONOSPHERE

by L. G. Smith, GCA Corporation, GCA Technology Division,
Bedford, Massachusetts

SUMMARY

This report describes an experimental investigation of the ionosphere using sounding rockets and is a sequel to earlier phases conducted during the International Quiet Sun Years. The payload instrumentation and objectives are described for each of the twenty-one launches, covering the period 14 June 1966 to 11 September 1969. The experimental program includes four launches in Brazil during and following the total solar eclipse of 12 November 1966; three in Puerto Rico in September 1967 in cooperation with the Arecibo Ionospheric Observatory; and fourteen launches at Wallops Island including investigations of the ionosphere at sunrise and of anomalous winter absorption. Results of these experiments are being published in the scientific literature.

I. INTRODUCTION

This program represents four years of ionosphere investigation using instrumented payloads. There have been 21 rocket flights with launch dates between June 1966 and September 1969. Four of these were launched in Brazil in a study of the total solar eclipse of 12 November 1966 and three were launched in Puerto Rico in September 1967 in a comparison of data with the Orecibo incoherent scatter radar. The other 14 were launched for Wallops Island in the course of eight field trips, representing a variety of scientific objectives.

The planning and execution of this program has been conducted in cooperation with the Aeronomy Laboratory, University of Illinois, represented by S.A. Bowhill, E.A. Mechtly, C.F. Sechrist, Jr. and G.W. Henry. The principal supporting personnel on the program have been P.J. McKinnon, L.H. Weeks, F.A. Lane, E.P. King, L.J. Johnson, C.G. Arouchon, G.A. Pintal and F.X. Brennan. In addition the cooperation and support provided by the Sounding Rocket Branch, NASA/GSFC and the NASA Wallops Station in the administrative and operational aspects of the program is gratefully acknowledged. The NASA Project Scientist has been E.R. Schmerling, NASA Headquarters, without whose support this program would not have been possible.

Section II contains descriptions of the scientific objectives of the flights, the experiments developed and used in the payloads and the performance of the vehicles and instrumentation. Reference is made to other

publications, many of which are now published in scientific journals, for details of the results of these investigations. Table 1 gives a listing of published papers and presentations and scientific meeting.

Section III of this report contains additional details of the instrumentation developed and used in the program. The development of the electron temperature probe is described separately, in Section IV.

A chrolonological list of the launches is given in Table 2. Three flights (14.272, 14.305, 14.309) were complete failures because of loss of telemetry signal or second stage ignition failure. Four (14.271, 14.273, 14.302, 14.393) were only partially successful because of failure of part of the instrumentation although some useful data were obtained. Fourteen flights were completely successful.

Table 1

PUBLICATIONS AND PRESENTATIONS ON CONTRACT NASW-1402

Publications

Bowhill, S.A.* and Smith, L.G., "Rocket Observations of the Lowest Ionosphere at Sunrise and Sunset," Space Res. VI, 511-521 (1966).

Smith, L.G., "Ionization by Lyman-α in the E region at Sunrise," J. Atmos. Terr. Phys. 28, 1195-1205 (1966).

Weeks, L.H., "Lyman-α Emission from the Sun Near Solar Minimum," J. Astrophys. 147, 1203-1205 (1967).

Mechtly, E.A.,* Bowhill, S.A.,* Smith, L.G., Knoebel, H.W.*, "Lower Ionosphere Electron Density and Collision Frequency from Rocket Measurements of Faraday Rotation, Differential Absorption and Probe Current," J. Geophys. Res. 72, 5239-5245 (1967).

Weeks, L.H. and Smith, L.G., "Molecular Oxygen Concentrations in the Upper Atmosphere by Absorption Spectroscopy," J. Geophys. Res. 73 4835-4849 (1968).

Smith, L.G., Weeks, L.H., and McKinnon, P.J., "Rocket Observations of Electron Temperature in the E Region," J. Atmos. Terr. Phys. 30, 1301-1312 (1968).

Mechtly, E.A.* and Smith, L.G., "Growth of the D Region at Sunrise," J. Atmos. Terr. Phys. 30, 363-369 (1968).

Mukunda Rao, M.* and Smith, L.G., "Sporadic E Classification from Rocket Measurements," J. Amtos. Terr. Phys. 30, 645-650 (1968).

Weeks, L.H. and Smith, L.G., "A Rocket Measurement of Ozone Near Sunrise," Planet. Space Sci. 16, 1189-1195 (1968).

Mechtly, E.A.* and Smith, L.G., "Seasonal Variation of the Lower Ionosphere at Wallops Island during the IQSY," J. Atmos. Terr. Phys. 30, 1555-1561 (1968).

Smith, L.G., "Langmuir Probes in the Ionosphere," in Small Rocket Instrumentation Techniques, ed. K.I. Maeda, North Holland Publishing Co. (1969).

*University of Illinois

Table 1 (Continued)

Mechtly, E.A.*, Seino, K.,* and Smith, L.G., "Lower Ionosphere Electron Densities Measured During the Solar Eclipse of November 12, 1966," Radio Sci. 4, 371-375 (1969).

Smith, L.G., "A Sequence of Rocket Observations of Nighttime Sporadic E," J. Atmos. Terr. Phys. 32, 1247-1257 (1970).

Mechtly, E.A.* and Smith, L.G., "Changes of Lower Ionosphere Electron Densities with Solar Zenith Angle," Radio Sci. (in press).

Presentations

Smith, L.G.: "Ionization by Lyman-α in the E-region at Sunrise," COSPAR, Vienna (May 1966).

Weeks, L.H., Smith, L.G. and McKinnon, P.J.: "Molecular Oxygen Densities from 70 to 154 km During Solar Minimum," AGU, Los Angeles (September 1966).

Smith, L.G. and Weeks, L.H.: "Rocket Observations of Electron Temperature in the E-Region," URSI, Ottawa (May 1967).

Weeks, L.H. and Smith, L.G.: "A Rocket Measurement of Ozone at High Altitudes," AGU, Washington, D.C. (April, 1969).

Smith, L.G., Weeks, L.H., and McKinnon, P.J.: "Rocket Observation of Electron Temperature in the E-Region," COSPAR, London (July, 1967).

Mechtly, E.A.,* Seino, K.,* and Smith, L.G.: "Lower Ionosphere Electron Densities Measured During the Solar Eclipse of 12 November 1966," URSI, Washington, D.C. (April, 1968).

Smith, L.G., "Langmuir Probes in the Ionosphere," COSPAR, Tokyo (May, 1968).

Smith, L.G., "Rocket Observations of Ozone above 50 km," COSPAR, Prague (May, 1969).

Weeks, L.H. and Smith, L.G., "Lyman-α Measurements During the Solar Eclipse of 12 November 1966," AGU, San Francisco

*University of Illinois

Table 2

ROCKET LAUNCHES, CONTRACT NASW-1402

Nike Apache	Time LST	Date	Place*	Remarks
14.270	0418:30	14 Jun. 1966	W.I.	$\chi = 94^{o}$
14.271	1815	24 Aug. 1966	W.I.	$\chi = 85^{o}$
14.272	1945	24 Aug. 1966	W.I.	TM failure
14.274	1106	12 Nov. 1966	Brazil	eclipse
14.302	1108	12 Nov. 1966	Brazil	eclipse
14.304	1110	12 Nov. 1966	Brazil	eclipse
14.303	1300	12 Nov. 1966	Brazil	post-eclipse
14.275	1350:35	31 Jan. 1967	W.I.	$\chi = 60^{o}$
14.273	1856	8 Aug. 1967	W.I.	$\chi = 90^{o}$
14.308	1634:22	7 Sep. 1967	P.R.	$\chi = 60^{o}$
14.305	2007	7 Sep. 1967	P.R.	TM failure
14.309	0603	8 Sep. 1967	P.R.	vehicle failure
14.358	0506	24 Jul. 1968	W.I.	$\chi = 90^{o}$
14.359	0536	24 Jul. 1968	W.I.	$\chi = 85^{o}$
14.360	1200:30	24 Jul. 1968	W.I.	noon
14.361	1736	24 Jul. 1968	W.I.	$\chi = 60^{o}$
14.391	1200	31 Jan. 1969	W.I.	$\chi = 55^{o}$
14.392	1209	6 Feb. 1969	W.I.	$\chi = 53^{o}$
14.393	1600	17 Apr. 1969	W.I.	partial instr. failure
14.395	1546	10 Sep. 1969	W.I.	$\chi = 60^{o}$
14.394	2306	11 Sep. 1969	W.I.	night

* W.I. = Wallops Island, Virginia ($37^{o}50'N$, $75^{o}29'W$)

Brazil = Cassino, R. G.du Sol ($32^{o}12'S$, $52^{o}10'W$)

P.R. = Vega Baja, Puerto Rico ($18^{o}34'N$, $66^{o}28'W$)

II. EXPERIMENTAL PROGRAM

A. General

This section summarizes the scientific objectives of the individual flights or groups of flights and specifies the instrumentation and any special circumstances. The performance of vehicle and instrumentation is also noted.

B. Nike Apache 14.270

Flight Objectives. - This flight was a further investigation of the initial development of the ionosphere in the D region shortly before ground sunrise. Previous observations had indicated that the illumination of the region by solar radiation in the UV, rather than in the visible part of the spectrum, was responsible for the initial increase of electron density in the C layer, at about 65 km. This agrees well with the onset of VLF absorption at a solar zenith angle (χ) of about 96°. On some days the onset of VLF absorption is observed at $\chi \approx 98^{\circ}$ corresponding to illumination by visible radiation. The specific purpose of Nike Apache 14.270 was to observe the properties of the D region and to determine, if possible, the cause of the anomaly in VLF absorption. The payload, Type A Mod. 3, included three main experiments: CW propagation, DC/Langmuir probe and solar radiation (Lyman-α and 2600A). This was the first time that a 2600A detector had been included in the payload and the first flight of the log-differential probe. The propagation and probe experiments are used in combination to obtain an electron density profile with good height resolution. In addition, the propagation experiment gives electron collision frequency in the D region while the probe gives electron temperature in the E region. The absorption profiles of Lyman-α and 2600A radiation give the concentration profiles of molecular oxygen and ozone, respectively, over limited ranges of altitude in the D region.

This payload also included an ion-bombardment experiment. Ion-bombardment, in vacuum, is a technique for removing contamination from the surface of an electrode. The precise mechanism is not known, but probably involves local heating of the surface. The specific reason for including this experiment was to further study the apparent anomaly in electron temperature: most rocket-borne probes have indicated electron temperature in the E region significantly greater than the neutral temperature. It was believed that ion-bombardment would lead to an evaluation of the role of surface contamination as a cause of the high electron temperatures. For a period of 40 seconds, near apogee, the nose-tip electrode was disconnected from the probe. During this period, a potential of -600 volt was applied to the nose-tip.

Performance. - The vehicle was launched on 14 June 1966, from Wallops Island. It was the fifth attempt to obtain the necessary ionospheric conditions. The vehicle performance was good; that of the instrumentation also good, except for delayed ejection of the door covering the ozone photometer. Data were, however, obtained from this experiment on the descending part of the trajectory.

C. Nike Apaches 14.271 and 14.272

Flight Objectives. - A series of three launches was planned as a study of the day-to-night transition of the E region. The launch times were chosen to give solar zenith angles of 85°, 102° and 112°, respectively. The first time would correspond with the E region still in photo-equilibruim with the solar radiation. The second time, with a geometrical shadow height of 144 km, would represent the E region immediately after the removal of radiation. The third flight represents a further interval of 55 minutes. The decrease in electron density allows the value of the effective recombination coefficient to be determined. The value had been shown by eclipse observations to be at least 1×10^{-7} cm^3 sec^{-1}, but laboratory studies indicate even higher values for the dissociative recombination of NO^+, the predominant night time ion.

The instrumentation of the first and third rockets (14.271 and 14.273) comprised a quadrupole positive-ion mass-spectrometer (designed by C. D. Hendricks, University of Illinois), in addition to the propagation and probe experiments. The latter consisted of a fixed potential on the nose-tip electrode; the data end with the ejection of the nose cone at an altitude of about 90 km. This payload (Type C, Mod. 1) is described in Section IV.

The second payload (Type B, Mod. 2) of the series included two boom-mounted probes, in addition to the propagation and probe experiments. One of the booms carried a spherical ion trap (supplied by A. F. Nagy, University of Michigan) while the other was instrumented with an electron temperature probe, adapted from an instrument devised by R. L. F. Boyd and A. P. Willmore and based on the analysis of M. J. Druyvesteyn. The development of the electron temperature probe is described in Section IV.

Performance. - The operation was scheduled for 24 August 1966 and the first launch took place at 1815 LST ($\chi = 85°$). The performance of this vehicle was satisfactory. The nose cone ejected at T+80 sec (91 km) and power was applied to the mass spectrometer at T+85 sec (96 km). Noise was observed for a few seconds on the signal from the mass spectrometer, but this died down and what appeared to be ion mass peaks were observed.

The second rocket (Nike Apache 14.272) was launched on schedule, 90 minutes later, at 1945 LST. Again, the vehicle performance was satisfactory. At the time of first stage burn out (T+3.5 sec) the transmitter power suddenly decreased by 40 db and the telemetry signal became noisy. The experiment appeared to be working perfectly, however, and some data were subsequently obtained from the DC probe up to an altitude of about 90 km. The telemetry signal returned to essentially full strength for a period of 14 seconds, starting at T+127 seconds, giving some additional data in the altitude range 138 to 148 km, on ascent.

The sequence of data had been broken and further study of the data from the mass spectrometer threw doubt on the quality of the data. The operation was cancelled and the third rocket (Nike Apache 14.273) was not launched.

D. Nike Apache 14.274, 14.302, 14.304 and 14.303

Flight Objectives. - This operation represents participation in NASA expedition to Southern Brazil for the total solar eclipse of 12 November 1966. The launch side was at Cassino, Rio Grande du Sol.

The principal scientific objective in the E region was the determination of the positive ion composition at totality and the comparison with the uneclipsed condition. This was to be accomplished by launching a payload containing a quadrupole position ion mass spectrometer into the region of totality and the second, about two hours later, when the ionosphere has recovered its normal condition.

The principal objective in the D region was a study of the role of photodetachment. The method was to compare the electron density profiles just before and just after totality. An additional objective was the observation of the residual flux of Lyman-α, because of its importance as a source of ionization in the D region.

Four primary flights were prepared and, in addition, two more flights were included as back-up for launch in the event of failure of any of the primary vehicles. The six payloads on their vehicles, shortly before the eclipse, are shown in Figure 1, which also includes the seventh rocket of the NASA program: an attempt to measure motion of the neutral atmosphere by photography of a TMA trail. The planned and actual launch times of the seven vehicles are given in Table 3.

The modification to the Type C payload, subsequent to the first unsuccessful flight on Nike Apache 14.271, consisted in lengthening the quadrupole elements of the mass spectrometer and, additionally, modifying

Figure 1. NASA eclipse expedition, Cassino, R.G. du Sol, Brazil.

Table 3

NASA ECLIPSE EXPEDITION

Nike Apache	Payload	Planned Time	Actual Time
14.77	TMA/Probe	1402 UT	1402 UT
14.274	Type A Mod. 4	1406	1406
14.302	Type C Mod. 2	1408	1408
14.304	Type A Mod. 4	1410	1410
14.305	Type C Mod. 2	1600	Not launched
14.275	Type A Mod. 4	Back-up	Not launched
14.303	Type A Mod. 4	Back-up	1600

the structure to include an EUV electrometer experiment (supplied by F. de Mendonca, Brazil).

The Type A payload was modified for the eclipse in that the solar radiation experiment comprised photometers for Lyman-α and 1450A, except that on 14.303 a photometer at 1300A was substituted for the 1450A photometer. All three detectors are used to obtain the concentration profile of molecular oxygen, over different rangesof altitude. The solar aspect sensors were adapted to the conditions of low light levels. An operational amplifier was added and measurements of aspect angle made with a solar flux of 0.1 percent of that from the unobserved sun

The Type A payload was also changed to improve reliability and simplify operational procedures: the door release mechanism was redesigned and an electronic timer substituted for the mechanical timer that had been used in all previous Type A payloads. The mechanical timer was retained in the Type C and later Type B payloads, but the new release mechanism was incorporated into these payloads.

Performance. - The launch operation in Brazil was coordinated with two other groups (DASA and LASL) launching from adjacent areas.* In all, fifteen rockets were launched during and immediately following the eclipse. It is to the credit of those involved in the operation that all rockets were launched on time, all vehicles performed satisfactorily and generally good telemetry signals were recorded.

The first four rockets of the NASA program were launched at the planned times, between 1402 and 1410 UT. The vehicles performed satisfactorily as did the instrumentation, with the exception of the positive ion mass spectrometer. No spectra were obtained although the monitors indicated proper functioning of the payload, including ejection of the nose cone at T+89 sec (102 km) and application of power to the mass spectrometer at T+98 sec (111 km). It was therefore decided that the second mass-spectrometer payload should not be launched and that the first back-up, Nike Apache 14.275, should be substituted. However, the solar radiation experiment did not show the proper response on closure of the calibration relay. It was later found that the battery supplying -15 volt to the electrometers had discharged, though no cause was found. The second back-up, Nike Apache 14.303, was prepared for launch and the operation was completed, largely successfully, at the planned time. The two unused payloads (14.275 and 14.305) were brought back from Brazil for later use.

*An illustrated article describing the overall operation, written by C. A. Accardo, is published in Sky and Telescope, February 1967.

The eclipse circumstances at the rockets are represented in Figure 2. These are computed from the tabulated radar trajectories. The numbers plotted are: (1) the area of the solar disc as a percentage of the unobscured disc and (2) for these parts of the trajectory that the vehicle is in totality, the interval since second contact at that position in space.

Nike Apache 14.274 ascends through the D region with about 3 percent of the disc visible. It enters totality at an altitude of 93.5 km on descent. At 70 km on descent, that point has been in totality for about 30 sec. Nike Apache 14.302 enters totality at 81.5 km on ascent and emerges from totality at 157.5 km, shortly after passing its apogee. Nike Apache 14.304 entered totality shortly after launch and emerges at 83.5 km on ascent. At 70 km, that point has been in totality for about 110 sec. During descent through the D region, about 5 percent of the disc is visible. These circumstances are very close to those specified for the launches.

E. Nike Apache 14.275

Flight Objectives. - This flight was planned as a further study of anomalons winter absorption. The particular objective on this occasion was an investigation of the relationship of electron density and (neutral) temperature in the D region. The latter quantity was to be obtained from two rocket launches using the grenade technique (J. Theon, NASA/GSFC). The first of these was planned to follow the ionosphere experiment by 10 minutes, the second was to be launched a few days later when the absorption had returned to normal values. The criterion for launch was established in terms of the absorption, measured at vertical incidence, on a frequency of 3030 kHz.

The payload (Type A, Mod 4) was modified from that brought back from Brazil by the substitution of a 2600A photometer in place of the 1450A photometer.

Performance. - The required condition of high absorption occurred on the first day that launch was attempted. Nike Apache 14.275 was launched at 1350:35 LST on 31 January 1967. The performance of vehicle, telemetry and instrumentation was good, although the signal level from the 2600A photometer was only about 10 percent of the expected value. The absorption profile at this wavelength was obtained, but the accuracy of the ozone concentrations determined from it is reduced. No satisfactory explanation of the low signal amplitude has been devised.

The associated grenade experiment on Nike Cajun 10.207 was launched at 1411 LST and gave satisfactory data. The second grenade experiment

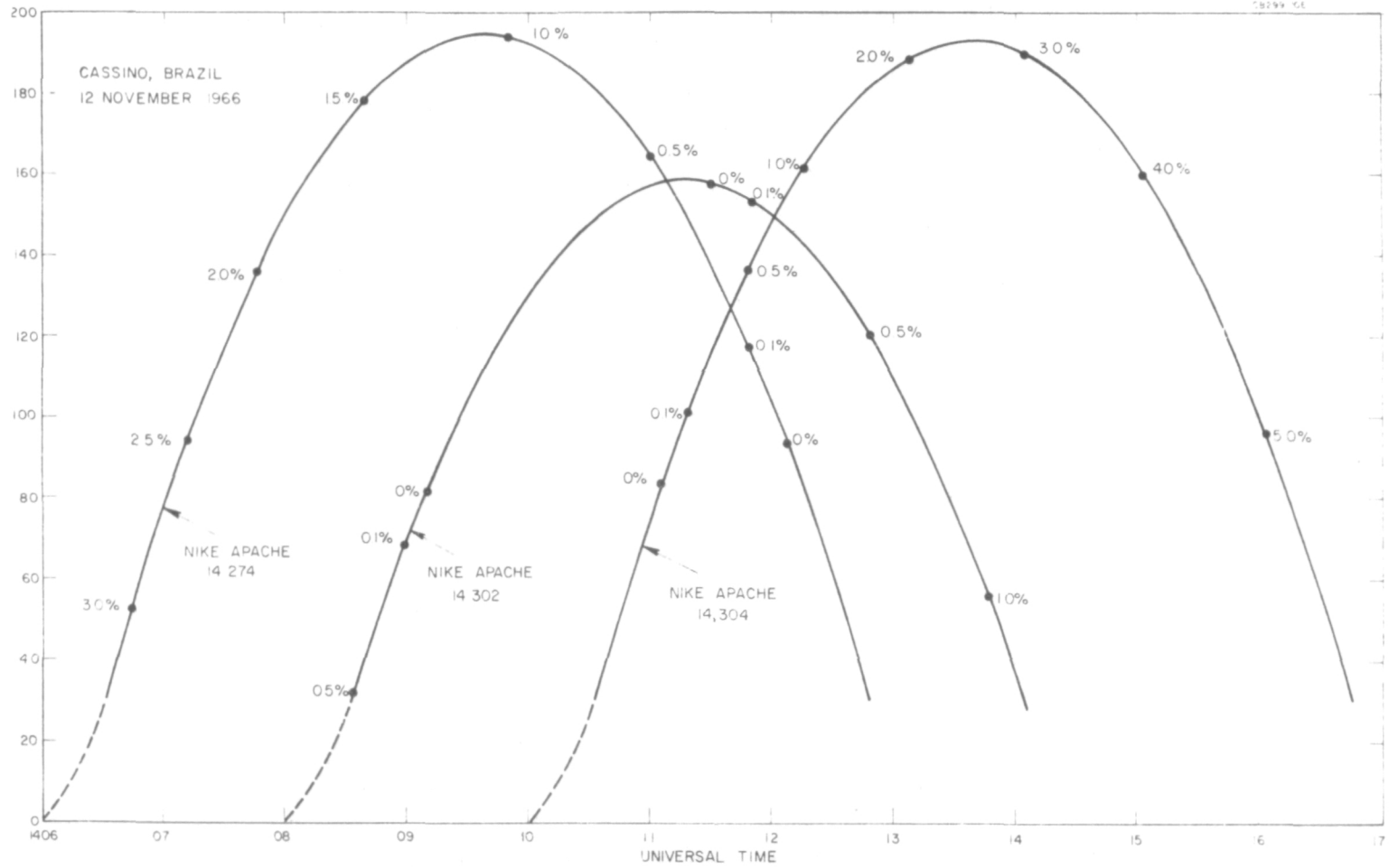

Figure 2. Eclipse circumstances at the rocket position: s = seconds since second contact, % = area of disc visible.

on Nike Cajun 10.222, for normal absorption condition, was launched at 1252 LST on 3 February 1967 and also gave good data.

F. Nike Apache 14.273

Flight Objectives. - This flight was planned as an investigation of non-blanketing sporadic-E. It also served as a further test flight of the positive ion mass spectrometer. The payload (Type C Mod. 2), had been on a back-up rocket (14.305) in Brazil and included the EUV electrometer experiment. The DC probe was arranged to measure the current to the nose tip electrode until the nose cone was ejected to expose the mass spectrometer. After ejection of the nose cone, the positive ion current to the first aperture plate of the mass spectrometer was measured by the probe electrometer. This served the double purpose of monitoring the performance of the mass spectrometer and of providing a current profile for the electron density profile. Other modifications had been made in the spectrometer in an attempt to eliminate problems which had invalidated two earlier launches (14.271 and 14.302). The vehicle was changed to a Nike Cajun (10.247) in order to reduce the vehicle velocity in its passage through the region of sporadic E (maximum expected altitude 120 km). Later modifications increased the weight of the payload to the extent that the vehicle was changed to a Nike Apache (14.273) in order to ensure adequate peak altitude.

The criterion for launch was established by ionisonde observation as fbEs $\leq$ 3MHz and foEs $\geq$ 4MHz. The launch window was 1700 to 1900 LST.

Performance. - The launch was accomplished on the first attempt. The time was 1856 LST on 8 August 1967 and the ionosphere conditions met the criteria given above. The probe data confirms the penetration of the sporadic-E layer. The altitude is 102 km both on ascent and descent. The passage through the layer, on ascent, occurred after nose-cone ejection (93 km), but before the turn-on of the mass-spectrometer (107 km).

The performance of vehicle and instrumentation were satisfactory, again with the exception of the mass spectrometer. No ion mass spectra were obtained, but no specific malfunction in the instrument or elsewhere in the payload has been found.

G. Nike Apaches 14.305, 14.308 and 14.309

Flight Objectives. - The primary objective of the series of flight was comparison of electron density and electron temperature data obtained from rocket-borne instrumentation with that obtained by incoherent scatter radar, located at the Arecibo Ionosphere Observatory in Puerto Rico.

A temporary launch site was established at Vega Baja, about 50 km from the observatory. Launch times were chosen to represent daytime (afternoon), nighttime (after sunset) and sunrise conditions at solar zenith angles of 60°, 110° and 92°, respectively. If possible, the launches were to be accomplished, in this sequence, within a period of about 14 hours.

The payload for the daytime and sunrise flight (Nike Apaches 14.308 and 14.309, respectively) were Type A, Mod. 4, as flown during the Brazil eclipse, with the solar radiation experiment using photometers for Lyman-α and 2600A. The payload for the nighttime flight (Nike Apache 14.305) had been built for Nike Apache 14.273 for the launch planned for 24 August 1966, but had been set aside when problems developed in the mass spectrometer. It was decided that there was no justification for further development of this instrument and that the payload would be of more value if converted to accommodate boom-mounted probes. It became a Type B, Mod. 3 payload. The two booms carried the same types of probes that had been included in the payload of Nike Apache 14.272: the spherial ion trap, (supplied by A. F. Nagy, University of Michigan) and the Boyd-Willmore version of the Druyvesteyn probe.

Performance. - The first launch was accomplished successfully on 7 September 1967. Nike Apache 14.308 was launched at 1634:22 LST. The launch had been delayed by the presence of shipping in the off-shore impact area and the solar zenith angle at the rocket at an altitude of 90 km was subsequently computed to be 62.4° on ascent and 63.2° on descent.

The second flight (Nike Apache 14.305) followed at 2007 LST, also on 7 September 1967. The vehicle performance was good. The telemetry signal was lost at launch; it recovered at first stage burn-out (T+3.5 sec), but was lost again at second stage ignition (T+23.7 sec). It recovered at second stage burnout (T+30.2 sec), but the modulation ended at T+56.2 sec, although the carrier continued to T+142 sec. The signal, with modulation, returned at T+339 sec and continued until the vehicle impacted at T+383 sec. No usuable signal was received during the time the payload was in the ionosphere and consequently the flight is considered a complete failure.

The subsequent flight (Nike Apache 14.309) launched at 0603 LST on the following morning (8 September 1967) also failed to give any useful scientific data. In this case the second stage failed to ignite and the maximum altitude attained was about 20 km. The instrumentation performed satisfactorily during the brief flight.

H. Nike Apache 14.358, 14.359, 14.360 and 14.361

Flight Objectives. - The general purpose of scheduling four launches in a single day was the study of the duirnal variation of the ionosphere in the D, E and F1 regions, covering the altitude range 50 to 200 km. The principal properties observed were electron density, electron temperature and electron collision frequency, and the concentration profiles of molecular oxygen and ozone. The particular launch times were selected to complement and extend previous observations which have been obtained in studies of the development of the ionosphere at sunrise and, on other other occasions, the seasonal and latitudinal variation of the daytime ionosphere (usually at $\chi=60^{o}$). The four times were selected for solar zenith angles of 90^{o} and 85^{o} (morning), 18^{o} (noon) and 60^{o} (afternoon).

The potential value of these four flights was considerably enhanced by cooperation of other experiments interested in this region of the atmosphere. Three groups were able to arrange flights for the same day. These were: J. B. Pearce, University of Colorado, with a day airglow experiment measuring nitric oxide concentration; W. S. Smith, NASA/GSFC, with a grenade experiment for atmospheric temperature and ensity measurements; and J. W. Peterson, University of Michigan, with a falling sphere experiment, measuring atmospheric density. The entire sequence of eleven launches in a period of 21 hours is given in Table 4 with actual launch times and approximate values of solar zenith angle.

The payloads (Type A, Mod. 5) for the ionosphere experiments are nearly identical. All contain the propagation and probe experiments and a solar radiation experiment. Each payload includes two UV detectors, one of which is for Lyman-α; in 14.358 and 14.359 the other is for 2600A and in 14.360 and 14.361 the other is for 1350A.

Performance. - All rockets in the series were launched within a few minutes of the scheduled times and, as far as can be determined, all the experimenters obtained the major portion of their expected data.

The first three rockets with ionosphere experiments were late by 1 min, 6 min and 30 sec, respectively, with the fourth exactly on time. All vehicles and instrumentation performed satisfactorily. The axis of the precession cone of 14.360 was inclined at only 10^{o} to the rocket-sun line, compared with the expected angle of 25^{o}. This resulted in

Table 4

ACTIVE SUN LOWER IONOSPHERE PROGRAM

Vehicle*	Date	LST	X**	Experiment
14.349	23 Aug 1968	1919	91°	Airglow
10.258	23 Aug 1968	1946	94	Grenade
10.253	24 Aug 1968	0000	115	Sphere
14.348	24 Aug 1968	0454	91	Airglow
14.358	24 Aug 1968	0506	90	Ionosphere
10.265	24 Aug 1968	0519:18	89	Grenade
14.359	24 Aug 1968	0536	85	Ionosphere
14.360	24 Aug 1968	1200:30	18	Ionosphere
10.254	24 Aug 1968	1345	26	Sphere
14.361	24 Aug 1968	1636	60	Ionosphere
10.266	24 Aug 1968	1655	64	Grenade

*Prefix 10. = Nike Cajun; 14. = Nike Apache

**Approximate value of solar zenith angle

the sun not being visible to the UV photometers for about 50 per cent of each precession period. The extinction profiles obtained on ascent and on descent can be combined to give a nearly complete concentration profile of molecular oxygen.

I. Nike Apache 14.391 and 14.392

Flight Objective. - The interest generated by the previous rocket studies of anomalous winter absorption provided the stimulus for the cooperative program which included these two flights. Scientists known to be interested in the altitude range of 50 to 120 km were convassed as to their interest in participating in such a program. The following scientific promised active participation in the rocket launches.

R. S. Narcisi, AFCRL, positive-ion concentration using a pumped quadrupole mass spectrometer;

L. G. Meira, University of Colorado, nitric oxide concentration by the UV airglow technique;

J. S. Theon, NASA/GSFC, pressure, density and temperature of the neutral atmosphere using the grenade experiment;

J. F. Morrissey, AFCRL, neutral density by the falling sphere method;

A. J. Krenger, NOTS, ozone concentration by absorption spectroscopy;

D. F. Heath, NASA/GSFC, nitric oxide airglow polarization measurements.

The cooperation of the Meteorological Rocket Network was arranged by W. L. Webb.

The following ground-based radio experiments were included in the program:

G. W. Henry, University of Illinois, vertical incidence absorption at 3.03 MHz;

A. J. Ferraro and H. S. Lee, Pennsylvania State University, absorption and wave-interaction at 2.2 MHz and 3.4 MHz;

J. S. Belrose, Communications Research Center, Ottawa, partial-reflection soundings;

G. D. Falcon and E. V. Thrane, ESSA, Boulder, partial reflection soundings;

R. H. Doherty, ESSA, Boulder, LF phase and amplitude measurements on Nantucket-to-Florida path.

Two series of rocket launches were scheduled: the first day selected to represent anomalous absorption. The criterion for characterizing the day was based on the vertical incidence absorption measurement at 3.03 MHz, at Wallops Island. The payloads of Nike Apache 14.391 and 14.392 were Type A, Mod. 5, with the photometers of the solar radiation experiment measuring Lyman-α and 2600A.

Performance. - The first series of launches, for the anomalous day, took place on 31 January 1969 between 1200 and 1653 LST. The second series, for the normal day, was launched on 6 February 1969 between 1209 and 1609 LST. The sequence of 13 launches on the two days is given in Table 5. Two flights, AH 7.573 and 14.396, both on the first day, yielded no data, but the remaining flights including Nike Apache 14.391 and 14.392 were completely successful in performance of both vehicle and instrumentation.

The first day was anomalous, based on the 3.03 MHz absorption measurement at Wallops Island. It also appeared anomalous at Pennsylvania State University, but at Ottawa and Boulder the absorption was determined to be normal.

The second day was normal by the criterion established for the 3.03 MHz absorption. The observations at Boulder, Ottawa and Pennsylvania State University, however, all characterize this day as anomalous. The rocket data, particularly that of the propagation experiment, also indicate that 6 February 1969 was an anomalous day. It appears that both days of the Specimen Day Program were anomalous. The misidentification provided by the 3.03 MHz absorption measurement at Wallops Island has since been found to be caused by deviative absorption in the lower E region.

J. Nike Apache 14.393

Flight Objectives. - A series of rocket launches had been conducted on Quarterly World Days in the years 1964 and 1965 as part of the program for the International Quiet Sun Year. To complement these, additional launches have been planned for the period near solar maximum. Each launch is made at a solar zenith angle of 60° (nominal) generally in the afternoon. The recent flights of Nike Apache 14.391 and 14.392,

Table 5

SPECIMEN DAY PROGRAM

Vehicle	Date	LST	Experiment
14.391	31 Jan 1969	1200	Ionosphere
AH 7.891	31 Jan 1969	1230	Ion-composition
10.267	31 Jan 1969	1257:30	Grenade
15.61	31 Jan 1969	1321	Ozone
AH 7.573	31 Jan 1969	1336	Sphere
14.389	31 Jan 1969	1410	Airglow
14.396	31 Jan 1969	1612	Polarization
10.268	31 Jan 1969	1625	Grenade
AH 7.567	31 Jan 1969	1653	Sphere
14.392	6 Feb 1969	1209	Ionosphere
15.62	6 Feb 1969	1300	Ozone
14.390	6 Feb 1969	1429	Airglow
10.296	6 Feb 1969	1609	Grenade

represent winter data. The summer observation is represented by Nike Apache 14.361. Nike Apaches 14.393 and 14.395 are the completion of this series, representing spring and fall conditions.

The payload (Type A, Mod. 6) for this flight incorporated two independent propagation experiments. All previous flights had used a single frequency for the propagation experiment; most commonly 3385 kHz for the daytime launches and 2225 kHz for other times (sunrise, sunset and night). The frequency chosen represented a compromise in the altitude range over which the electron density profile could be obtained by the two methods of data analysis; differential absorption and Faraday rotation. A smaller frequency would favor lower altitudes and a greater frequency would favor higher altitude. It was decided to modify the experiment to extend the altitude range by using two frequencies. Those selected for the first flight were 2225 and 5040 kHz. Two separate receivers, each with its own antenna were incorporated in the redesigned payload. The mechanical arrangement of the assembly was adapted from a circularly polarized antenna system developed for flight at the magnetic equator (Nike Apache 14.228). In addition to the two-frequency propagation experiment the payload included the DC/Langmuir probe experiment and the solar radiation experiment with photometers for Lyman-α and 2600A.

Performance. - The launch took place at 1600 EST on 17 April 1969*. The performance of the vehicle was satisfactory and a good quality telemetry signal received. A partial failure occurred in the instrumentation resulting in loss of data from the probe and solar radiation experiments. Neither propagation experiment was involved and both gave good data. The cause of the partial failure has been determined to be the failure of the 70 kft baroswitch to actuate. Since this is used to end the calibration sequence which had been initiated by the 40 kft baroswitch, the probe and solar radiation experiments remained in the calibrate mode for most of the flight. The baroswitch had been tested and found to be operating satisfactory before the flight. As a result of this experience the baroswitches in subsequent flights have been made redundant.

The successful operation of the propagation experiments accomplished the primary objective of a spring-time measurement at solar maximum.

---

*Note that the date has been erroneously quoted as 16 April 1969 in some reports.

K. Nike Apache 14.395

Flight Objectives. - This flight was intended to complement the previous Launch (Nike Apache 14.393) and give data on the lower ionosphere on a fall day at solar maximum

The payload (Type A, Mod. 6) was identical with that of Nike Apache 14.393, except for the inclusion of redundant baroswitches to avoid the possibility of recurrence of the problem encountered in the earlier flight.

Performance. - The vehicle was launched from Wallops Island at 1546 LST on 10 September 1969. The vehicle performance was satisfactory, although the impact range was much smaller than predicted, indicating a high effective launch elevation angle: intended as 83°, it appeared to be 87°. This high angle is advantageous for the experiments, but is considered unacceptable by the range for reasons of safety. The instrumentation all operated satisfactorily and good quality data were obtained.

L. Nike Apache 14.394

Flight Objectives. - The structure of the nighttime ionosphere (to 200 km, say) has been revealed by rocket flights to be at least as complex as that of the daytime ionosphere, but has not yet been investigated to the same degree. The opportunity arose, on the initiative of S. M. Radicella, Argentina, to make simultaneous observations from Wallops Island and from Chamical, Argentina.

The payload (Type B, Mod. 4) included the propagation experiment using a single frequency (2225 MHz) and the DC/Langmuir probe. In addition, the booms were used in an experiment to determine the ratio of mobility of positive and negative ions in the D region, at altitudes at which the contribution of free electrons to the probe current is negligible. The upper limit of the measurements was expected to be 80 km. The experimental method was relatively simple: the current to each electrode was measured as the potential of one switched between +22.5 volt and +4.05 volt and that of the other between -22.5 volt and -4.05 volt. The payload was also modified to monitor the firing of a mechanical delay igniter being developed by another contractor for use with Apache and Cajun motors. The field trip for this launch was combined with that of the preceding rocket, although the objectives are unrelated.

Performance. - Nike Apache 14.394 was launched from Wallops Island at 2306 LST on 11 September 1969. The Argentine rocket had been launched six minutes earlier. The performance of the Nike Apache was satisfactory, including that of the mechanical delay igniter (although the Apache itself was fired by the conventional pyrotechnic). The instrumentation performance was satisfactory. The data from the ion-mobility experiment presents problems of interpretation, though these are believed to be attributable to unanticipated shock wave effects.

The main objective, concerning the structure of the night time ionosphere, was achieved. The data show an example of the intermediate layer at night, a phenomenon which is now believed to be a regular feature.

M. Vehicle Performance

It has been noted in describing the individual launches that, with one exception (14.309) the performance of the vehicles has been satisfactory. More often than not, the apogee altitude has exceeded the predicted value. Aspects of vehicle performance which are immediately relevant to the experimental program are considered in Table 6, arranged by payload type and vehicle number. The value of apogee is obtained from the tabulated radar data. Two values are given for 14.274, 14.303 and 14.304 launched in Brazil. These rockets were tracked to about 100 km and the remainder of the trajectory generated by a vacuum extrapolation, giving the first value listed. The second value was obtained by applying a correction based on the observation of small sporadic-E layer and from the actuation times of the 70 kft baro-switches. The correction accumulates a difference in altitude at the following rates: 14.274, 6.3 m/sec: 14.303, 8.3 m/sec, 14.304, 21.3 m/sec.

The data on spin rate and the included angle and period of the precession cone are obtained from the aspect magnetometer, located transverse to the spin axis of the payload. The values are taken in mid-flight except for the Type B payload on Nike Apache 14.394. The two values given are the spin rates before and bollowing boom deployment at 52 km altitude. The nominal value of spin rate, obtained by attaching wedges to the firm of the second stage motor is 6 rps, the actual observed range of 5.2 to 9.5 rps represents the limitations of this method. The values are quite acceptable for the purposes of the experiments carried in these flights. There is some indication of an inverse relation between spin rate and precession cone period, but the magnitude of the included angle of the precession cone shown no such clear correlation with spin rate. Again, the range of values in the precessional motion is expected and acceptable. In fact, for the purpose of the solar radiation experiment, the precessional motion allows an in-flight aspect calibration of the detectors to be obtained while the vehicle is above the absorbing region for the particular radiation.

Table 6

SUMMARY OF ROCKET PERFORMANCE BY PAYLOAD TYPE

Payload Type	Vehicle	Apogee (km)	Spin Rate (rps)	Cone Angle (deg)	Period (sec)
Type A Mod 3	14.270	186.9	6.9	10.9	28.5
Mod 4	14.274	195.1/194.2	5.2	23.6	35.5
4	14.275	195.0	6.8	15.4	27.0
4	14.303	198.0/196.8	5.6	18.0	36.0
4	14.304	195.5/192.8	6.7	9.6	30.0
4	14.308	195.9	7.8	21.0	26.4
4	14.309	20.2	- - - - No Second Stage Ignition -		
Mod 5	14.358	213.4	7.3	4.2	28.9
5	14.359	212.9	7.1	23.8	29.0
5	14.360	215.6	8.0	20.3	26.0
5	14.361	209.8	6.5	17.6	32.5
5	14.391	225.2	7.6	10.8	27.6
5	14.392	218.9	9.5	19.5	22.0
Mod 6	14.393	206.7	7.1	24.9	30.5
6	14.395	213.4	6.3	18.8	35.0
Type B Mod 2	14.272	169.5	- No Data - - - - - - - - - - -		
Mod 3	14.305	150.5	- No Data - - - - - - - - - - -		
Mod 4	14.394	188.6	6.0/3.8	17.4	41.5
Type C Mod 1	14.271	164.1	5.6	16.6	38.5
2	14.273	141.5	6.3	10.0	44.0
2	14.302	158.2	5.2	10.7	27.3

III. INSTRUMENTATION

A. General

The complement of experiments used in the flight program has been briefly described in the previous section in terms of the scientific objectives. This section contains further details of the payloads and the instrumentation. Details of the experiments are not given here if they have appeared in the publications listed in Table 1. Variations which affect the construction and operational aspects of the payloads are described. The development of the electron temperature probe is described in a separate section.

Three types of payloads, in several modifications, have been employed. The propagation experiment and DC probe experiment have been carried on all payloads; the major differences between the three types of payload is represented by the additional experiments and the different construction involved. These are:

Type A: Solar radiation experiment; protected during the launch phase by ejectable doors.

Type B: Probes: deployed on booms, protected by ejectable doors.

Type C: Positive-ion mass-spectrometer; protected by ejectable nose-cone.

The construction of the payloads is based on a standard NASA Apache/Cajun design and uses plug-in assemblies and a wiring channel. The telemetry system has, in all cases, been FM/FM with 8 to 10 subcarrier oscillators and a four-element turnstyle antenna. The payloads have an aluminum shell and nose-cone, except for a non-metallic section at the location of the receiving antenna(s) of the propagation experiment(s). A complete Type A payload attached to its vehicle (Nike Apache 14.393) is shown on a military rail launcher in Figure 3. A "fly-away" umbilical connector, i.e., are which automatically disengages with first connected by the umbilical cable to the control console, Figure 4, located in the blockhouse. The signals at the inputs to the telemetry system may be selected at the console and displayed on the oscilloscope.

A switch permits a calibration signal to be applied to each experiment, where appropriate. Other switches control (1) the sweep of the DC/Langmuir probe; (2) the mechanical commutator, if used; (3) the transmitter, and (4) the power source between external and internal. An additional switch on the front and a second switch in series, on the

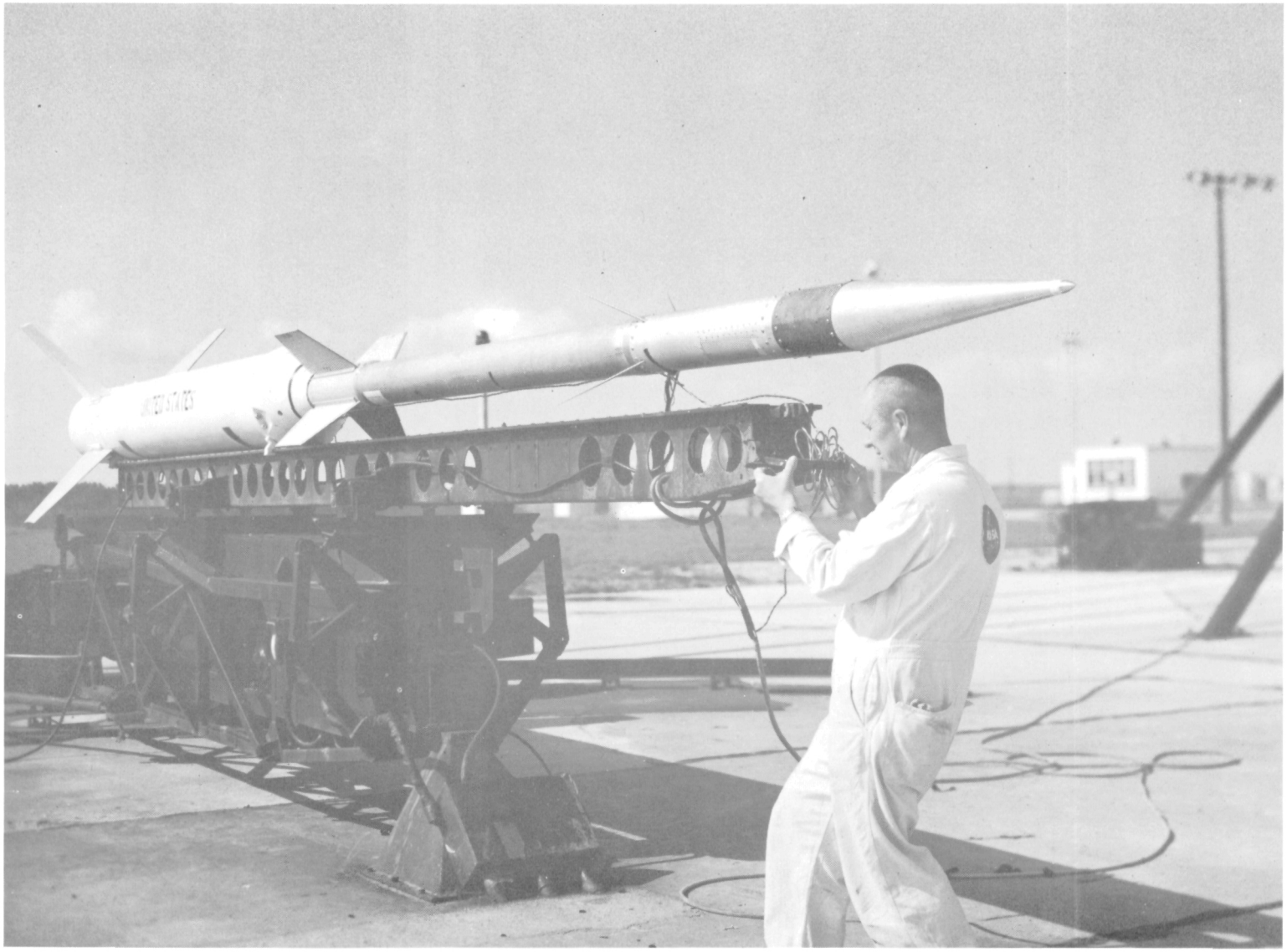

Figure 3. Nike Apache 14.393 on Launcher at Wallops Island

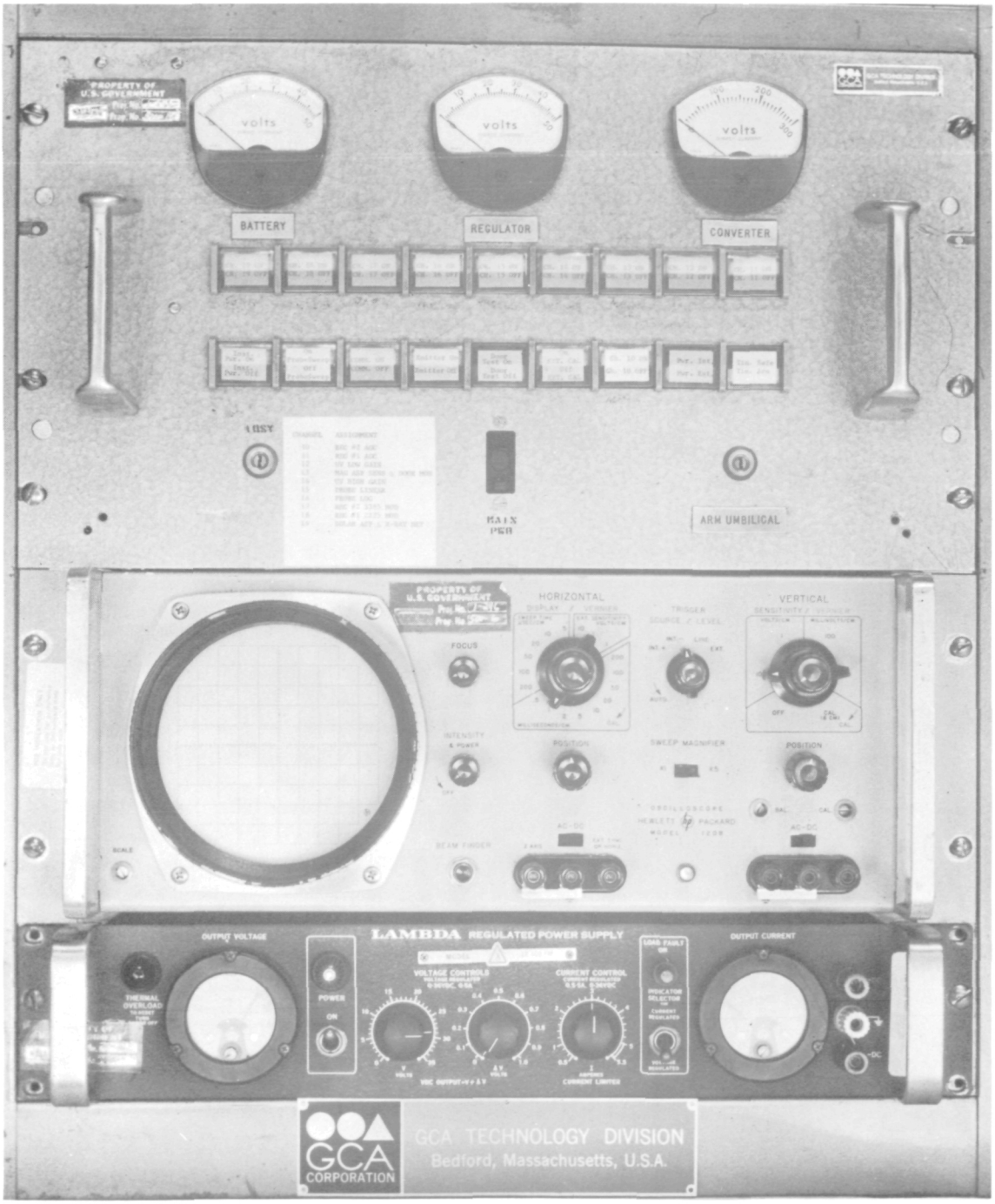

Figure 4. Payload control console.

back of the console arm the timers and allow the pyrotechnics to be fired during pre-launch checkouts. A light on the panel indicates the state of the timer: safe or armed. Meters on the upper part of the console indicate the voltage of the main payload battery and the voltage of the external power supply, at the payload; there may be a line drop one or two volts when a long umbilical cable is used. The meter for converter voltage is no longer required; it was used to monitor the voltage to a tube-type transmitter included in some earlier payloads. This method of controlling and continuously monitoring the payload up to the moment of launch has proved valuable and has contributed to the generally high level of successful flights in the program.

B. Type A Payloads

Four modifications of the Type A payload have been in the course of this program. Previous programs had used Mod. 1 (NASW-820) and Mod. 2 (NASW-1141)*.

Mod. 1 had been developed for the IQSY program.

Mod. 2, used on the CROATAN expedition to the South Pacific, involved changes in the control circuits: a latching relay replaced the motor-driven switch previously used for power transfer and an electronic timer replaced the mechanical unit in the door release circuit.

Mod. 3, used on only one flight (14.270), was the first to incorporate a newly developed DC/Langmuir probe (the log-differential probe). It also included the positive-ion bombardment experiment and, because of the multiple timing functions, reverted to a mechanical timer.

Mod. 4, shown in Figure 5, was developed for the Brazil eclipse operation and also used in the Puerto Rico expedition. It incorporated an improved door release mechanism. The electronic timer used on this and all subsequent Type A payloads was relocated adjacent to the released mechanism. The construction of the solar radiation experiment was also modified and improved ease of assembly.

Mod. 5, shown in Figure 6, is based on a major change in the payload structure. Previously, the umbilical connector and antenna had been separate from the main payload shell. The new design includes these as part of the main structure. Other changes were incorporated

*The final reports of these contracts contain descriptions and assembly drawings of these payloads.

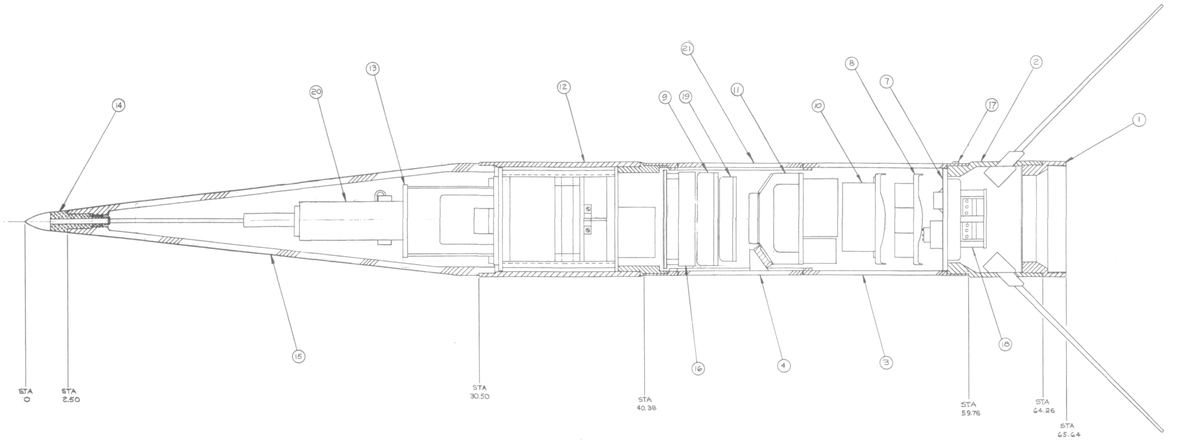

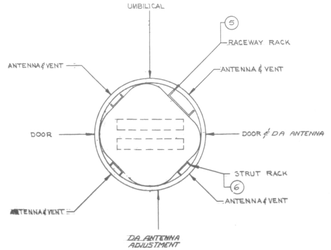

	D103811	INTERCONN. WIRING MODEL 4		REF
1	C102606	DOOR 4		21
1	C1079-9009	MAGNETIC ASPECT ASSEMBLY		20
1	C103689	+28 V BATTERY DECK		19
1	C102155	TRANSMITTER DECK ASSY		18
60	B1019-43	BOLT, BUTTON HEAD		17
1	D103733	DIAL DOOR RELEASE MECH		16
1	D102782	NOSE CONE 11" CAST		15

103833

1	C102471	NOSE PROBE ASSY		14
1	D102126	LANGMUIR PROBE MODEL XLP-10		13
1	D102106	DA RCVR ANTENNA ASSY		12
1	D102831	UV & SOLAR ASPECT DECK ASSY		11
1	D102154	BATTERY DECK ASSY		10
1	D103706	TIMER DECK ASSY		9
1	D102119	VCO DECK ASSY		8
1	D102157	CONTROL DECK ASSY		7
3	C102596	STRUT		6
2	D102826	RACEWAY-RACK		5
1	D103649	DOOR 3		4
1	R102624	SHELL A-PAYLOAD		3
1	D102776	ANTENNA SECTION ASSY		2
1	D102777	ADAPTER		1
QTY REQD	PART NO.	DESCRIPTION	SPECIFICATION	ITEM NO.

LIST OF MATERIAL

Figure 5. Payload Assembly, Type A Mod 4.

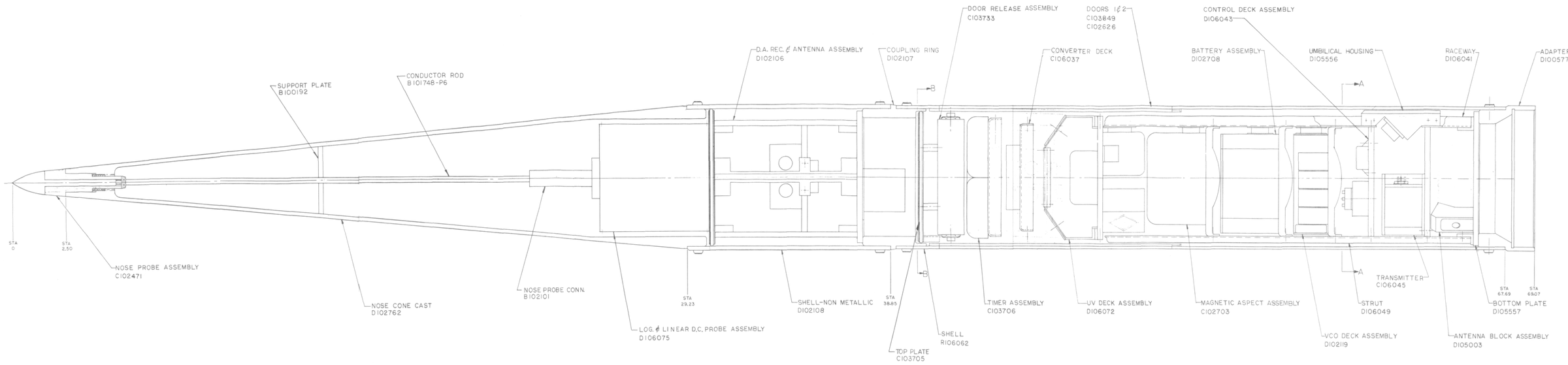

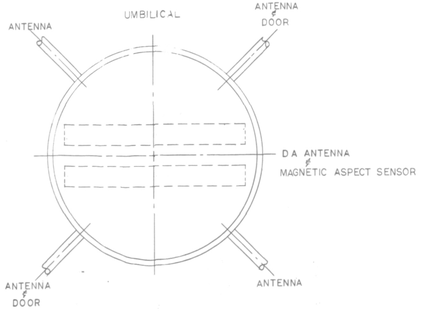

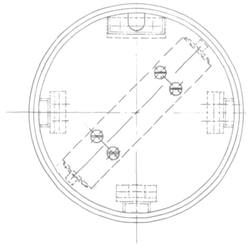

SECTION B-B

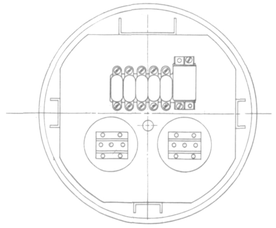

SECTION A-A

Figure 6. Payload Assembly, Type A, Mod 5.

in this modification. The bias supply (-15 volt) for the electrometers in the probe and UV experiments had previously been obtained from mercury batteries. The use of a converter had been avoided because of possible radio-frequency interference with the propagation experiment. In this and subsequent modifications, a negative voltage (-30 volt) is obtained from a DC-to-DC converter and reduced to -15 volt in each experiment. After some difficulty, proper RFI suppression of the converter was obtained. In this modification, the magnetometer was also relocated from the nose-cone to a position below the solar radiation experiment. This was done to eliminate some interaction between the probe electronic package and the magnetometer: relays in the probe package were introducing small errors in the magnetic aspect signal and the circuit of the probe. The type of transmitter used in the payload was also changed.

Mod. 6, the final version used in this program, differed from the preceding model in the replacement of the single frequency propagation experiment by a two-frequency experiment. The arrangement of the two mutually perpendicular antennas and the two receivers is shown in Figure 7. The change also increased the number of telemetry channels used in the Type A payloads from 8 to 10.

Several combinations of photometers have been used in the solar radiation experiment. In each case, one was an in-chamber sensitive to Lyman-α. Previous flights and the first flight (14.270) of the present program used for Lyman-α detection an ion chamber having a window of lithium fluoride (UF) and the fill gas of nitric oxide (NO). Subsequent flights have used a detector in which the window material is magnesium fluoride (MgF_2). There are two advantages to the change in material: (1) LiF absorbs a moisture film which slowly evaporates in flight, giving a change in sensitivity, whereas MgF_2 is not affected, and (2) the response of the LiF-NO ion chamber is 1050-1350A, that of the MgF_2-NO ion chamber 1120-1350A. Thus, the contribution of unwanted radiation is reduced.

The second detector in each payload is given in Table 7. The 2600A detector consists of a phototube with a caesium-telluride cathode and a thin-film interference filter. The absorption profile of this radiation gives zone concentration. The 1300A detector is an ion chamber with a window of calcium fluoride (CaF_2) and a fill gas of nitric oxide. The detector is sensitive to radiation in the band 1225-1350A. It is used to provide a correction to the Lyman-α ion chamber, so that the oxygen concentration can be extended to greater altitudes. The 1450A detector is an ion chamber with a window of sapphire (Al_2O_3) and a fill gas of p-xylene. The detector is sensitive to radiation in the band 1425-1480A and gives oxygen concentrations up to about 150 km. The detector is used, in these flights, with gas gain, requiring a voltage of about 600 volt. The other detectors are braised with a small 45 volt mercury battery.

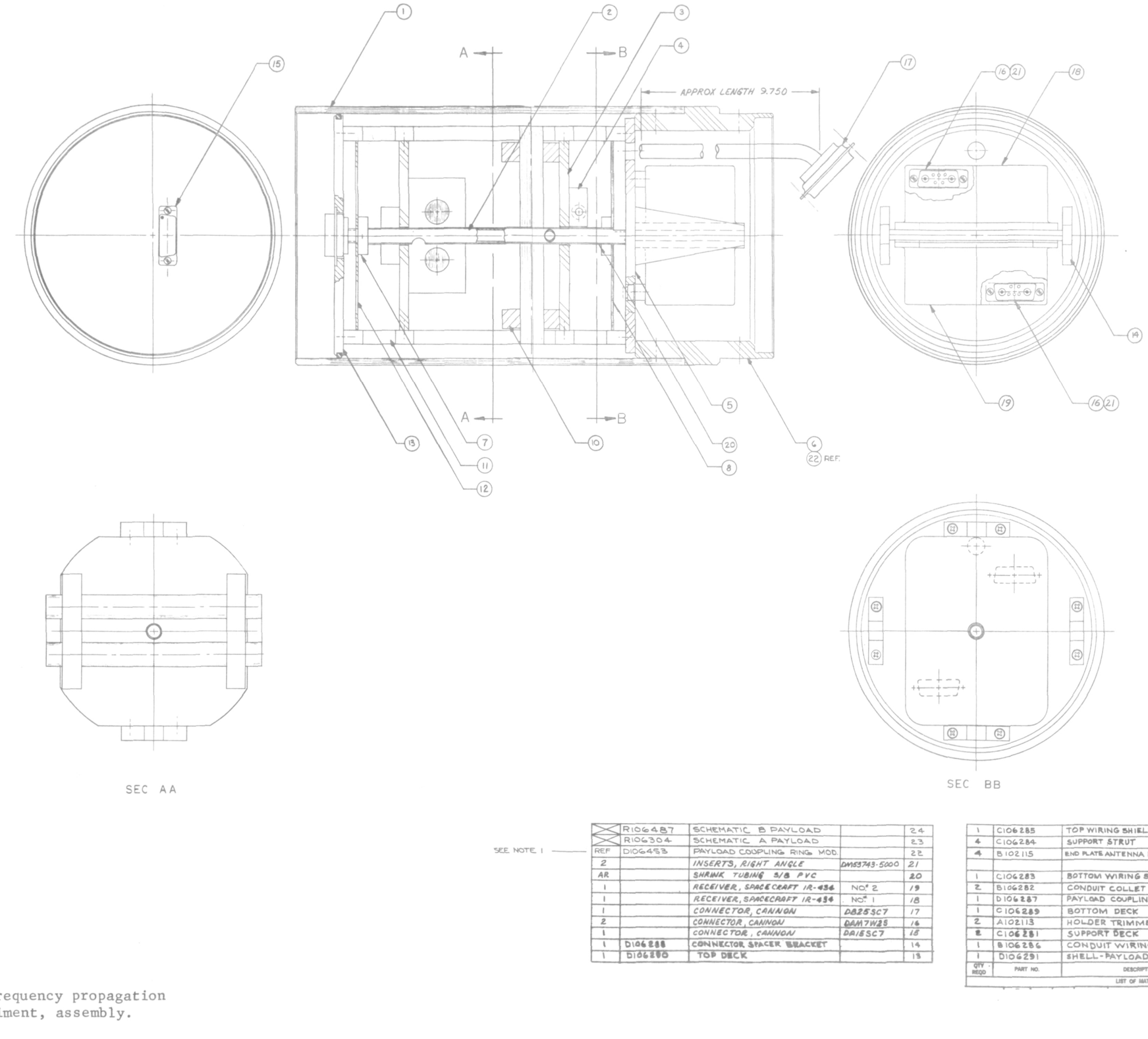

SEC AA

SEC BB

NOTES:

1. MODIFICATION TO COUPLING RING WHEN USED WITH 'B' PAYLOAD.

SEE NOTE 1

	R106487	SCHEMATIC B PAYLOAD		24
	R106304	SCHEMATIC A PAYLOAD		23
REF	D106453	PAYLOAD COUPLING RING MOD.		22
2		INSERTS, RIGHT ANGLE	DM53743-5000	21
AR		SHRINK TUBING 3/8 PVC		20
1		RECEIVER, SPACECRAFT IR-434	NO. 2	19
1		RECEIVER, SPACECRAFT IR-434	NO. 1	18
1		CONNECTOR, CANNON	DB25SC7	17
2		CONNECTOR, CANNON	DAM7W2S	16
1		CONNECTOR, CANNON	DA15SC7	15
1	D106288	CONNECTOR SPACER BRACKET		14
1	D106290	TOP DECK		13

106265

QTY REQD	PART NO.	DESCRIPTION	SPECIFICATION	ITEM NO.
1	C106285	TOP WIRING SHIELD		12
4	C106284	SUPPORT STRUT		11
4	B102115	END PLATE ANTENNA HOLDER		10
				9
1	C106283	BOTTOM WIRING SHIELD		8
2	B106282	CONDUIT COLLET		7
1	D106287	PAYLOAD COUPLING RING		6
1	C106289	BOTTOM DECK		5
2	A102113	HOLDER TRIMMER		4
8	C106281	SUPPORT DECK		3
1	B106286	CONDUIT WIRING		2
1	D106291	SHELL-PAYLOAD		1

LIST OF MATERIAL

Figure 7. Two-frequency propagation experiment, assembly.

Table 7

SOLAR RADIATION DETECTORS, TYPE A PAYLOADS

Vehicle	Detector	Remarks
14.270	2600A	Door ejected late
14.274	1450	
14.275	2600	
14.303	1300	
14.304	1450	
14.308	2600	
14.309	2600	No data
14.358	2600	
14.359	2600	
14.360	1300	
14.361	1300	
14.391	2600	
14.392	2600	
14.393	2600	No data
14.395	2600	

Note: All above vehicles included Lyman-α photometers.

C. Type B Payloads

Three payloads of this type were used in this program; one of each of three modifications; 2, 3 and 4. The payloads are generally adapted from the concurrent Type A modification.

Mod. 1, had been developed for the IQSY program, primarily to accommodate an RF probe supplied by J. Sayers, University of Birmingham*. Three flights used this Type B Mod. 1 payload.

Mod. 2 includes the electron temperature probe described in a later section. In other respects it is closely similar to the preceding modification.

Mod. 3 was generated by adapting a Type C Mod. 1 payload. The boom-probe assembly of Mod. 2 was mounted forward of the propagation experiments, as shown in Figure 8.

Mod. 4, shown in Figure 9, relocates the boom-probe assembly in its previous position, behind the propagation experiment. The main advantage is that fewer signals must be passed through the antenna assembly. This payload also incorporates the revised payload housing and the different transmitter.

D. Type C Payload

This payload incorporates a quadrupole positive-ion mass spectrometer and, in Mod. 2, an EUV electrometer experiment. Both instruments are located at the forward end of the payload behind an ejectable nose-cone with the apertures of both aligned with the spin axis of the vehicle. The nose-cone has an included angle of 20 degrees on this payload; on all Type A and most Type B payloads, the included angle is 11 degrees.

Figure 10 shows the assembly of the first version, Mod. 1. The mass spectrometer and its associated circuits occupy the payload forward of the coupling ring (item #15 on the drawing). The separate sub-assemblies consist of:

(a) Timer and rectifier;

---

* The assembly drawing of this payload is included in the final reports of Contracts NASW-820 and NASW-1141.

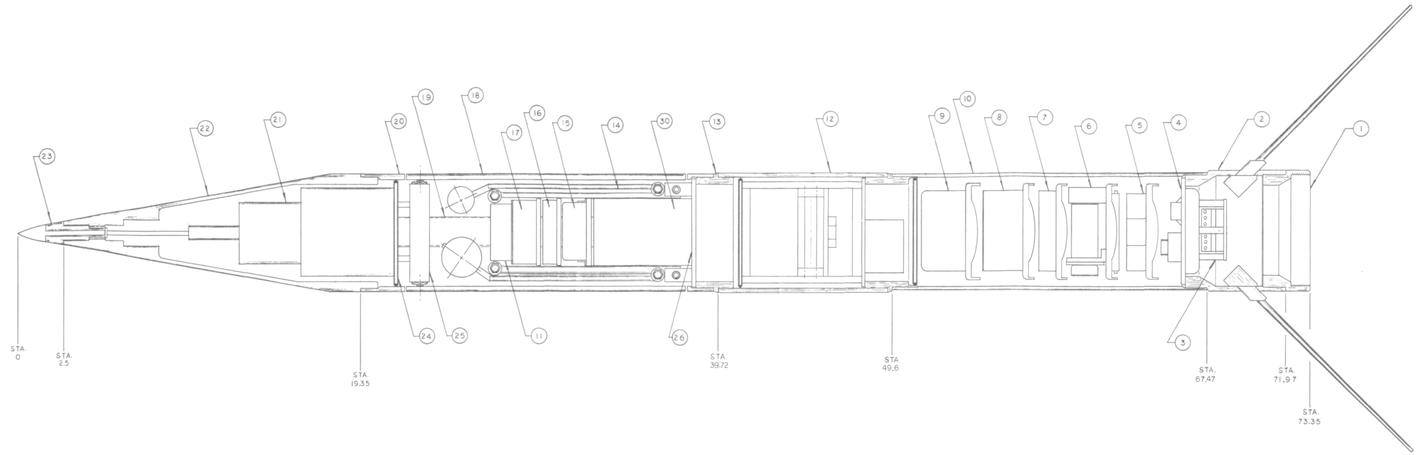

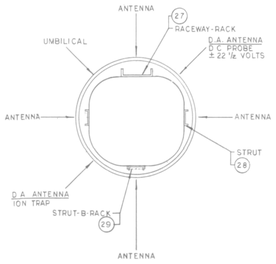

QTY REQD	PART NO.	DESCRIPTION	SPECIFICATION	ITEM NO.
		LIST OF MATERIAL		
116	B101543	BOLT, BUTTON HEAD		REF
><	R105023	INTERCONNECTION WIRING		REF
1	C000048	ION TRAP ELECT		30
1	C105262	STRUT		29
3	C102598	STRUT		28
1	D105690	RACEWAY		27
1	D104845	BOTTOM DECK-RACK		26
1	C103733	DUAL DOOR RELEASE MECH.		25
1	C105623	TOP DECK-RACK		24
1	C102471	NOSE PROBE ASSY		23
1	E104845	NOSE CONE 20° CAST		22
1	E105252	ELECTRON TEMP. EXP.		21
1	R105280	SHELL		20
1	D105261	RACEWAY		19
2	D105281	DOORS		18
1	D105313	LOG-LINEAR ELECTROMETER		17
1	D105301	PROBE TIMER		16
1	D105243	ELECTROMETER 3 RNG'S V		15
2	D105160	PROBE EXTENSION MECH.		14
1	D105662	COUPLING RING		13
1	D105106	DIFFERENTIAL ABSORPTION ASSY		12
		105293		
1	D105230	RAMP GENERATOR		11
1	R102699	SHELL		10
1	C102703	MAGNETIC ASPECT SENSOR		9
1	D102706	BATTERY DECK ASSY.		8
1	D102663	COMMUTATOR DECK ASSY.		7
1	C103642	TIMER DELAY DECK ASSY		6
1	D102179	V.C.O. DECK ASSY.		5
1	D102494	CONTROL DECK ASSY.		4
1	C102135	TRANSMITTER DECK ASSY.		3
1	D105576	ANTENNA SEC. ASSY		2
1	D105577	ADAPTER		1

Figure 8. Payload Assembly, Type B Mod 3.

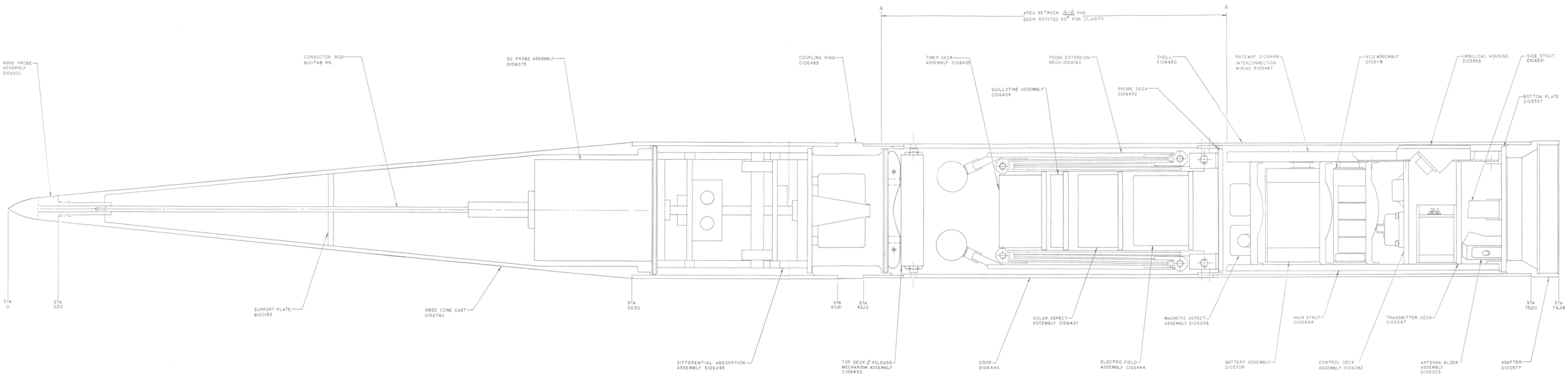

Figure 9. Payload Assembly, Type B
Mod 4.

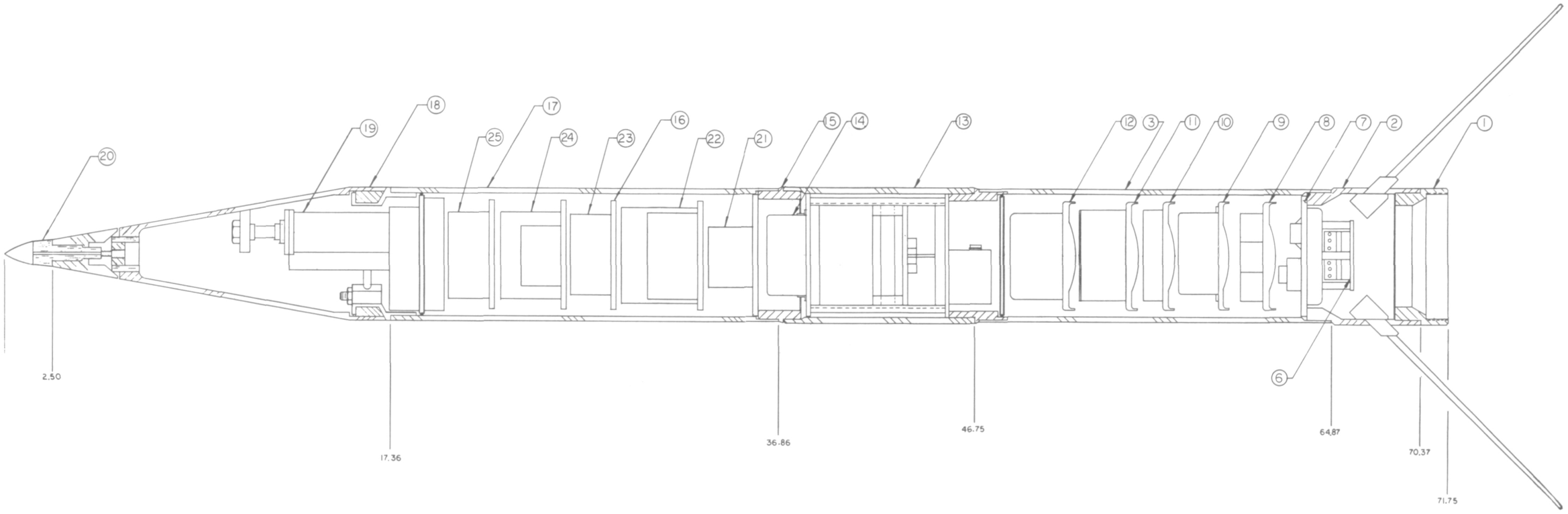

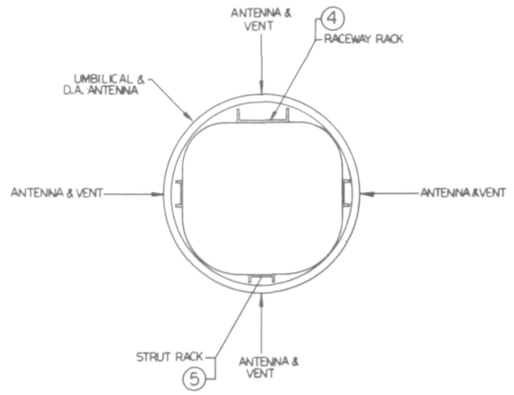

QTY REQD	PART NO.	DESCRIPTION	SPECIFICATION	ITEM NO.
		LIST OF MATERIAL		
1		TIMER & RECT. DECK		25
1		OSC. DECK.		24
1		LOG. AMP DECK		23
1		2000 V.D.C. POWER SUPPLY DECK		22
1		1000 V.D.C. POWER SUPPLY DECK		21
1	C102471	NOSE PROBE ASSY.		20
1	E102739	QUADRUPOLE MASS SPEC. ASSY		19
1	E102793	SPLIT NOSE CONE ASSY.		18
1	D102654	SHELL - MASS. SPEC.		17
1	E102663	RACK ASSY. MASS. SPEC.		16
1	D102662	COUPLING RING		15
1	C102787	ELECTROMETER ASSY		14
1	D102106	DIFFERENTIAL ABSORPTION RCVR. ANT. ASSY		13
				102655
1	C102703	MAGNETIC ASPECT SENSOR ASSY		12
1	D102708	BATTERY DECK ASSY		11
1	D102569	COMMUTATOR DECK ASSY		10
1	C102141	TIMER DELAY DECK ASSY		9
1	D102119	V.C.O. DECK ASSY		8
1	D102494	CONTROL DECK ASSY		7
1	C102135	TRANSMITTER DECK ASSY		6
3	C102698	STRUT RACK		5
1	D102690	RACEWAY RACK		4
1	R102699	SHELL C PAYLOAD		3
1	D100576	ANTENNA SECTION ASSY		2
1	D102577	ADAPTER		1

Figure 10. Payload Assembly Type C Mod 1.

(b) RF Oscillator (center frequency $\approx$ 2.5 MH_z) and ramp generator;

(c) High voltage power supply (2000 volt DC);

(d) Low voltage power supply (100 volt DC);

(e) Logarithmic electrometer.

The ions are detected by a multiplier (Bendix Model No. 306) having a gain of the order of 10^6. The output current of the multiplier is measured on a logarithmic electrometer, the output of which is telemetered on IRIB Channel 15. The ramp voltage is telemetered on IRIG Channel 12 and various monitor voltage are commutated and telemetered in IRIG Channel 19.

The circuit for the DC probe is contained within the coupling ring that joins the mass-spectrometer section to the propagation experiment. Up to the time of nose cone ejection, which occurs at an altitude of about 90 km, the insulated tip of the nose cone is used with the DC probe. The probe is used entirely in the DC mode, i.e., no sweep voltage, since no electron temperature data can be obtained in the D region.

The first model of the mass spectrometer was evacuated before launch to a pressure of 10^{-6} torr. This prevents contamination and reduces the time for out-gassing when the seal is broken at nose-cone ejection. The high voltage power supply is energized 5 seconds later.

The first flight, on Nike Apache 14.271, did not give ion mass spectra although all monitors indicated proper performance of vehicle and instrumentation. The instrument was modified, mainly in the assembly of the quadrupole elements, to eliminate some possible modes of failure. The revised version of the instrument is shown in Figure 11. The principal changes are:

(a) The sensitivity was increased by analyzing the diameters of the apertures of collector plate #1 and collector plate #2. The current to collector plate #1 was monitored by the circuit shown in Figure 12.

(b) The instrument was launched in the unsealed condition. Two vent holes were added, one to the quadrupole cavity and one to the multiplier cavity. These were arranged so that they could be plugged for pre-flight testing and calibration.

(c) The length of quadrupole rods was increased from 4.0 in. to 7.75 in. to improve resolution.

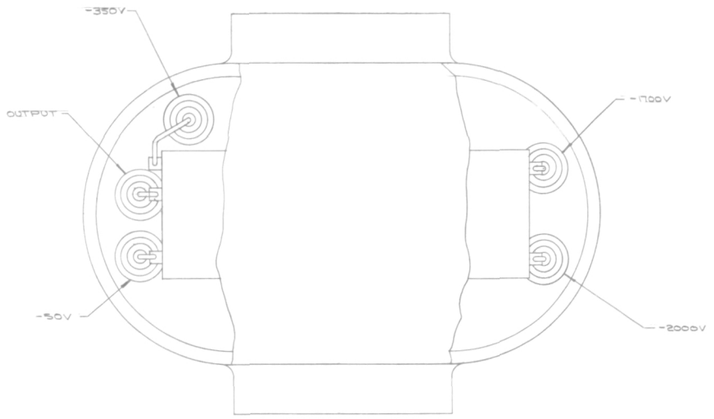

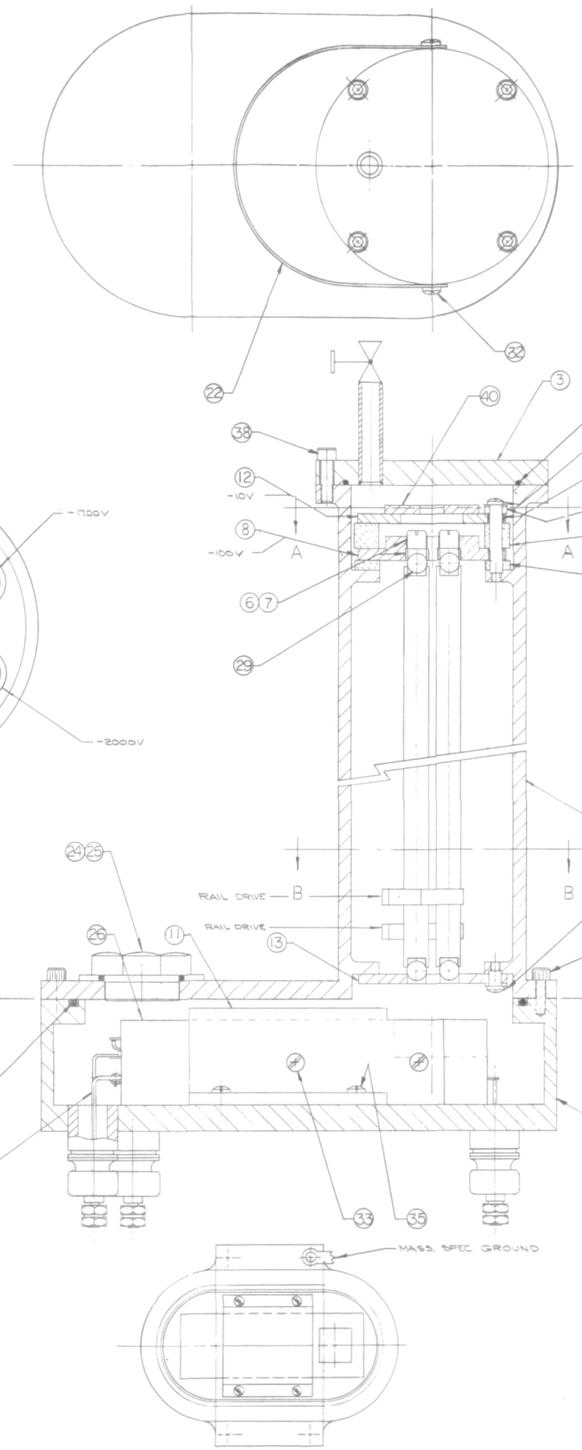

SECTION CC
SCALE 1/1

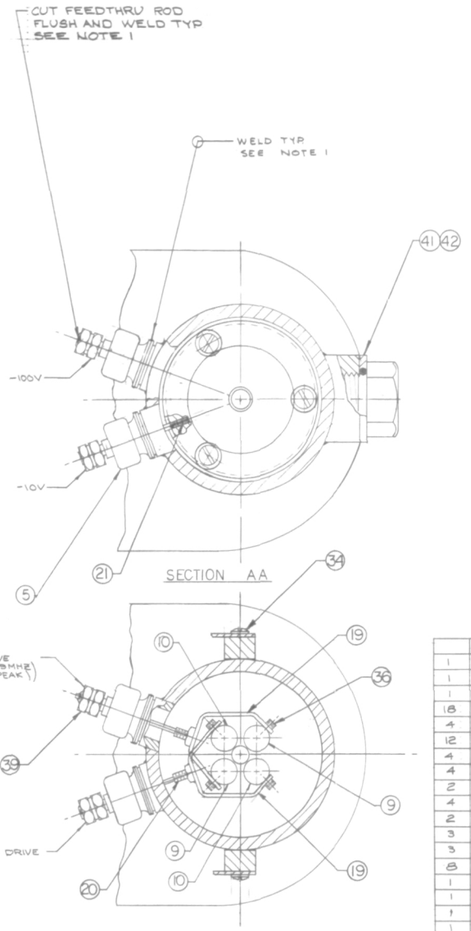

SECTION AA

SECTION BB

NOTES:
1. ALL WELDS TO BE TESTED PER G.C.A. STD B101.

QTY PER MOD	PART NO.	DESCRIPTION	SPECIFICATION	ITEM NO.
1	B103855	VENT PLUG "2		42
1		"STAT-O-SEAL PARKER	G00-018-112	41
1	B103853	COLLECTOR PLATE "1A		40
18		NUT, HEX. EXTRA SMALL PATTERN 4-32UNC-2B	CRES 18-8	39
4		SCREW, CAP, SOC HD, 4-40UNC-2A X 7/16 LG	CRES 18-8	38
12		SCREW, CAP, SOC HD, 4-40UNC-2A X 5/8 LG	CRES 18-8	37
4		SCREW, CAP, SOC HD, 2-56UNC-2A X 1/8 LG	CRES 304	36
4		SCREW, BINDER HD, 4-40UNC-2A X 5/16 LG	CRES 304	35
2		SCREW, BINDER HD, 2-56UNC-2A X 7/16 LG	CRES 18-8	34
4		SCREW, BINDER HD, 2-56UNC-2A X 5/16 LG	CRES 304	33
2		SCREW, BINDER HD, 2-56UNC-2A X 1/4 LG	CRES 18-8	32
3		WASHER FLAT "6	CRES 18-8	31
3		WASHER FLAT "4	CRES 18-8	30
8		BALL, RUBY SAPPHIRE 3/16 DIA	INDUSTRIAL TECTONICS INC.	29
1		O-RING	PARKER NO. 2-153 VITON	28
1		O-RING	PARKER NO. 2-120 VITON	27
1		MULTIPLIER	BENDIX MODEL NO. 306	26
1	B103854	VENT PLUG "1		25
1		STAT-O-SEAL PARKER	G00-016-3/4	24
3	C103742	WASHER INSULATOR		23
1	D103549	SHIELD		22
2	B103565	FEEDTHRU ROD NO. 2		21
2	B103564	FEEDTHRU ROD NO. 1		20
2	B103548	ROD CONNECTOR STRIP		19
3	B103520P2	SCREW		18
3	B103520P1	SCREW		17
8	B103521	INSULATOR		16
1	C103527	INSULATOR NO. 2		15
1	C103526	INSULATOR NO. 1		14
1	C103525	COLLECTOR PLATE NO. 2 MASS. SPEC.		13

102739

1	C103524	COLLECTOR PLATE NO. 1 MASS. SPEC.		12
1	C103535	MULTIPLIER BRACKET		11
2	C103522	COLLECTOR ROD NO. 2 MASS. SPEC		10
2	C103523	COLLECTOR ROD NO. 1 MASS. SPEC.		9
1	C103530	ADJUSTMENT PLATE		8
4	B103531	SPACER SLEEVE		7
4	B103532	ADJUSTMENT SCREW		6
4	B103550	MODIFIED FEEDTHRU		5
5	B103540	FEEDTHRU ROD NO. 3		4
1	C103538	REMOVABLE COVER		3
1	D103547	FINAL MACHINING QUADRUPOLE MASS. SPEC.		2
1	D103545	WELDMENT MULTIPLIER CAVITY		1

LIST OF MATERIAL

Figure 11. Assembly, quadrupole mass spectrometer, Mod 2.

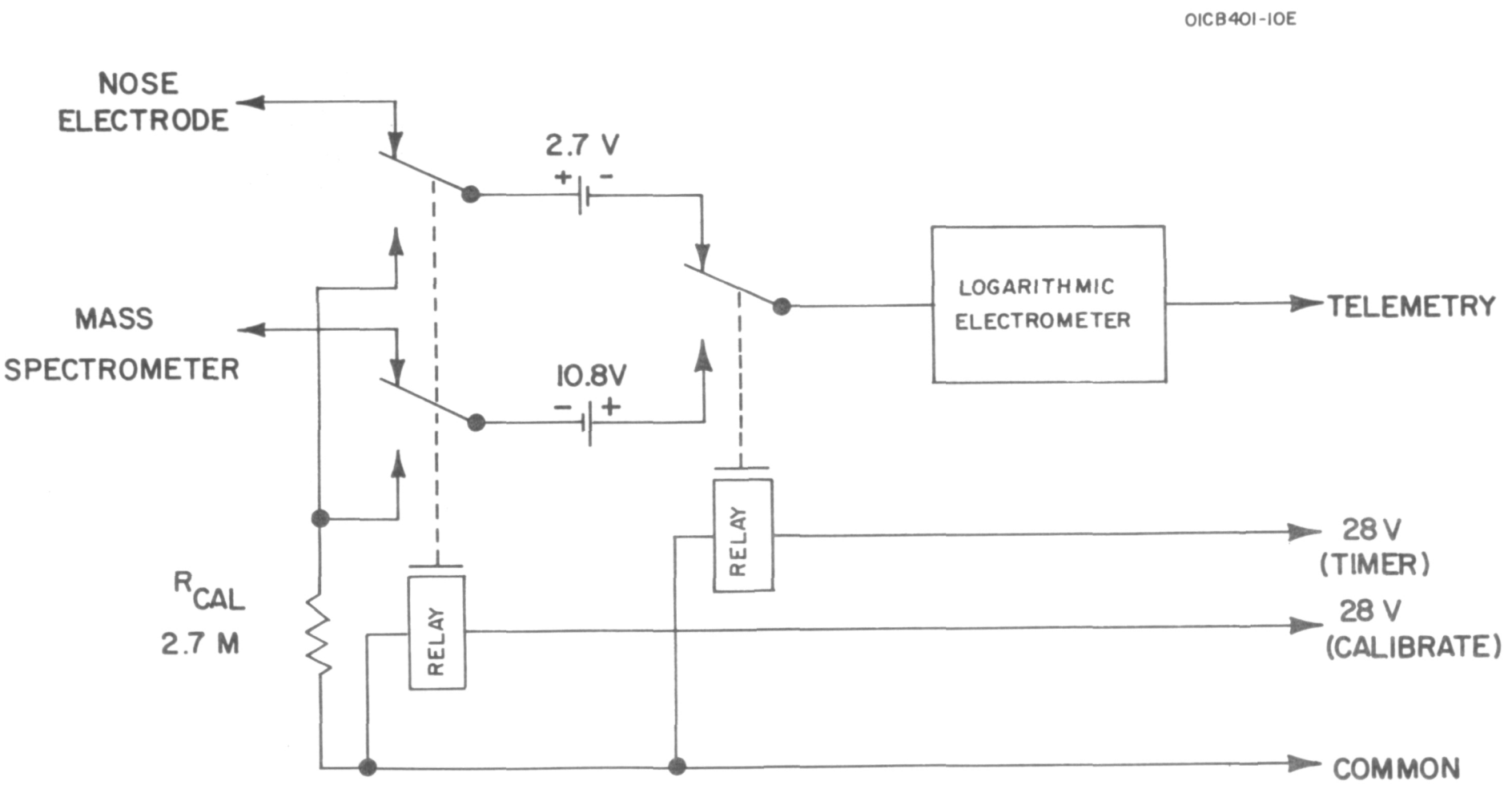

Figure 12. Probe and collector plate circuit schematic.

The assembly of the Type C, Mod. 2 payload is shown in Figure 13. This shows the increase in length of the split nose-cone assembly which was necessary to accommodate the modified mass spectrometer, and the EUV electrometer experiment.

Prior to each flight the mass-spectrometer section of the payload was tested and calibrated at the University of Illinois. Further tests of the complete payload were conducted in the Test and Environment Facility at NASA/GSFC. In spite of the extensive test procedures, the further flights of the experiment on Nike Apache 14.302 and 14.273 failed to give mass spectra although, again, all monitor voltages indicate proper operation of payload functions. After these disappointing results, the development of the payload was not continued.

E. Payload Construction

The method of construction of the payloads is illustrated in the following series of figures. The individual views may be identified in relation to the complete payload by reference to the appropriate assembly drawing given in the preceding pages.

The telemetry and control section, typical of the later Type A and Type B payloads, is shown in Figure 14. The base of the payload is the adapter which mates with the second stage motor. Above this, two of the four mounting blocks for the turnstyle antenna and their phasing network are visible. The next deck carries the telemetry transmitter. The umbilical connector, hidden from view by the transmitter, is attached to the wiring channel. The next higher assembly is the control deck. This contains the latching relay for power switching and two relays for switching the transmitter and the probe sweep circuit. Four additional relays disconnect signal and power leads from the umbilical connector to eliminate the possibility of a short-circuit in the event of damage to the connector on launch. The removal of voltages from the exposed pins of the connector is also desirable because of possible disturbance of the vehicle potential. The control deck also carries the baroswitches; two are shown, one for 40 kft and one for 70 kft; this was modified in later flights to two of each in a redundant circuit for increased reliability. The baroswitch assembly is made removable from the payload so that the baroswitches may be tested before flight and so that their function can be simulated in pre-flight checks by substitution of toggle switches.

The control deck also carries the mixer-amplifier of the telemetry system. The deck carrying the subcarrier oscillators, omitted in the picture, is located immediately above the control deck and mates with the connector visible in the wiring channel.

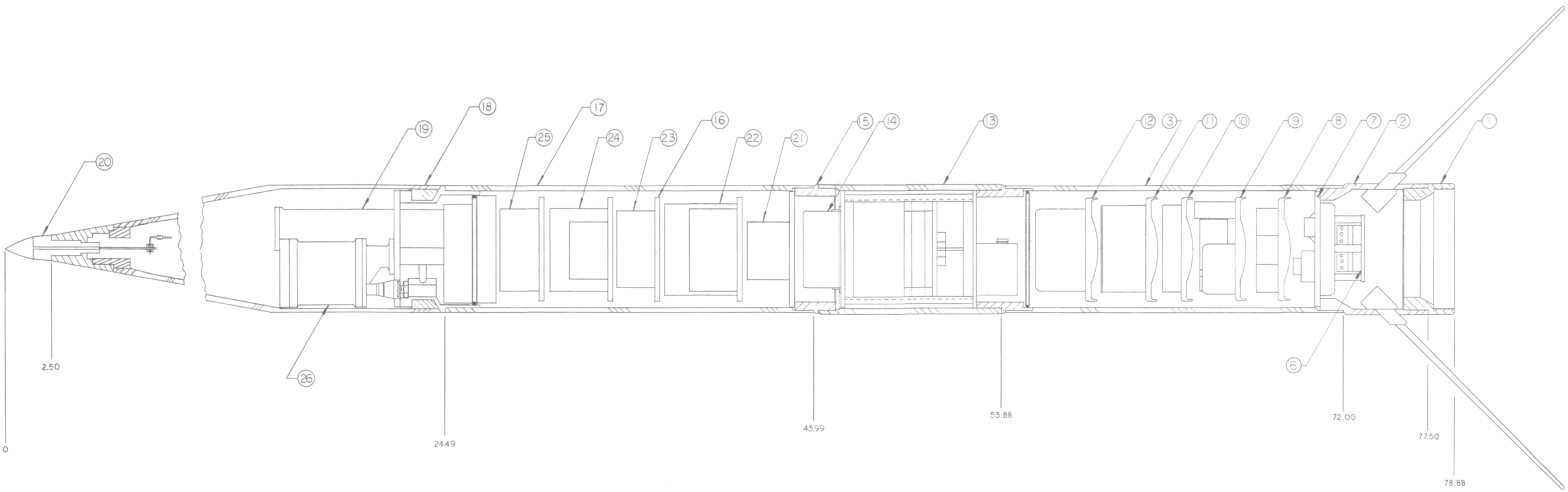

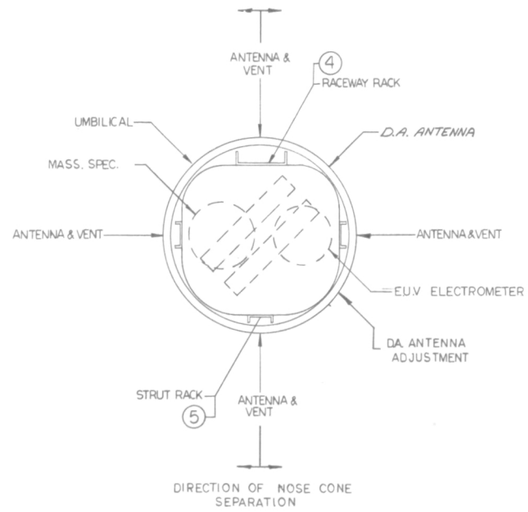

QTY REQD	PART NO.	DESCRIPTION	SPECIFICATION	ITEM NO.
	E102802	INTERCONN. WIRING MASS. SPEC. MOD. 2		REF.
	E102761	INTERCONN WIRING PAYLOAD C MOD.2		REF
1	C101	E.U.V. ELECTROMETER ASSY		26
1		TIMER & RECT. DECK		25
1		OSC. DECK.		24
1		LOG. AMP. DECK		23
1		2000 V.D.C. POWER SUPPLY DECK		22
1		1000 V.D.C. POWER SUPPLY DECK		21
1	C102471	NOSE PROBE ASSY.		20
1	E102739	QUADRUPOLE MASS SPEC. ASSY		19
1	R103796	SPLIT NOSE CONE ASSY		18
1	D102654	SHELL - MASS. SPEC.		17
1	E102663	RACK ASSY. MASS SPEC.		16
1	D102662	COUPLING RING		15
1	C102787	ELECTROMETER ASSY		14
1	D102106	DIFFERENTIAL ABSORPTION RCVR. ANT. ASSY		13
			103834	
1	C102703	MAGNETIC ASPECT SENSOR ASSY		12
1	D102708	BATTERY DECK ASSY		11
1	D102569	COMMUTATOR DECK ASSY		10
1	C103642	TIMER, DELAY DECK ASSY		9
1	D102119	V.C.O. DECK ASSY		8
1	D102494	CONTROL DECK ASSY		7
1	C102135	TRANSMITTER DECK ASSY		6
3	C102698	STRUT RACK		5
1	D102690	RACEWAY RACK		4
1	R102699	SHELL C PAYLOAD		3
1	D100576	ANTENNA SECTION ASSY		2
1	D102577	ADAPTER		1

Figure 13. Payload Assembly, Type C Mod 2.

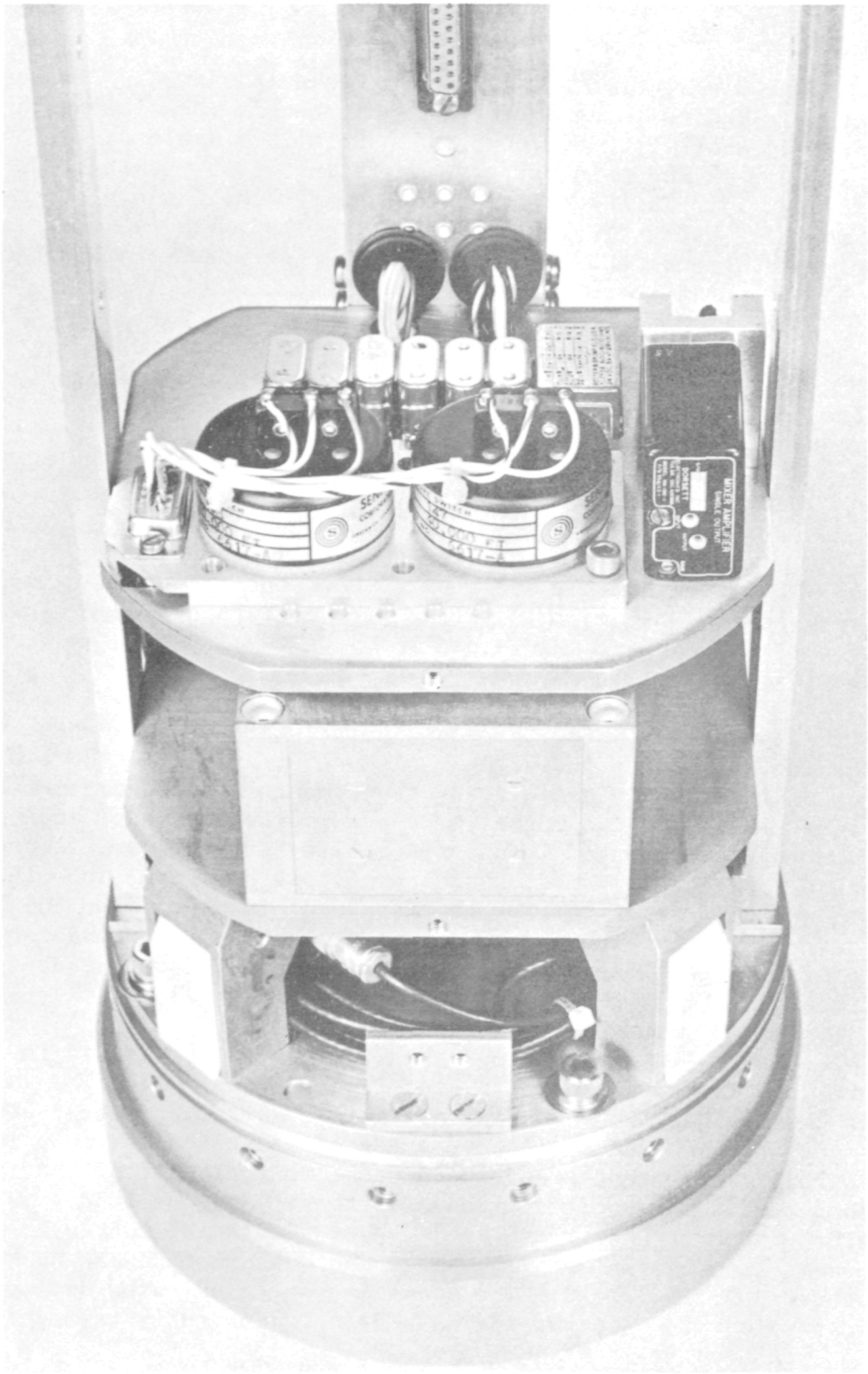

Figure 14. The telemetry and control section of the Type A Mod 6 payload.

The middle section of a Type A payload is shown in Figure 15. This is actually Mod. 6 (Nike Apache 14.393), but is identical with Mod. 5. Immediately above the SCO deck, and partially visible at the bottom of the picture, is the main battery consisting of 19 rechargeable cells (Yardney HR-1). This supplies all power for the payload, including the pyrotechnics, but excluding the biasing cells (mercury) used in the experiments. Above the battery is the aspect magnetometer (Schonstedt Type RAM-5C) on a non-metallic deck.

The deck containing the solar radiation experiment is located in the middle of the picture. The two photometers, diametrically opposed and inclined at an angle calculated to give the best view of the sun, are located on the upper side of the deck with the bias battery (-45 volt). The electrometer and amplifier for these detectors are mounted on the lower side of the deck, together with the solar aspect sensor.

The next higher deck contains the regulated DC-to-DC converter, output -30 volt. A metal cover was subsequently added for additional RFI suppression. Above this is the deck containing the electronic time delay for the door-release mechanism which completes this section of the payload.

The lower section of the payload is joined to the upper section by a coupling ring, seen in the next picture, Figure 16. The two receivers of the dual-frequency propagation experiments are contained within the coupling ring. The two mutually perpendicular antennas, each using two ferrite rods are mounted in a non-metallic structure and is contained within a non-metallic section of the payload housing. The electronics package of the DC/Langmuir probe experiment is mounted on the top deck of the propagation experiment assembly. The special connector at the top of the picture mates with the rod descending from the nose-tip electrode.

The general arrangement of the Type B, Mod. 4 payload is shown in Figure 17. The shell and nose-cone have been removed. The photograph is of the payload flown on Nike Apache 14.394 which omits one of the propagation experiments. At the stage of construction shown in the photograph, the antennas and the probe electronic circuit had not been encapsulated. The booms are shown in the folded position. They are retained by a wire which is severed by a guillotine cutter to deploy the booms from the spinning rocket. The construction of the booms is illustrated in Figure 18. The booms are designed to be deployed at a vehicle spin rate of 6 rps and have been successfully tested at 7.2 rps.

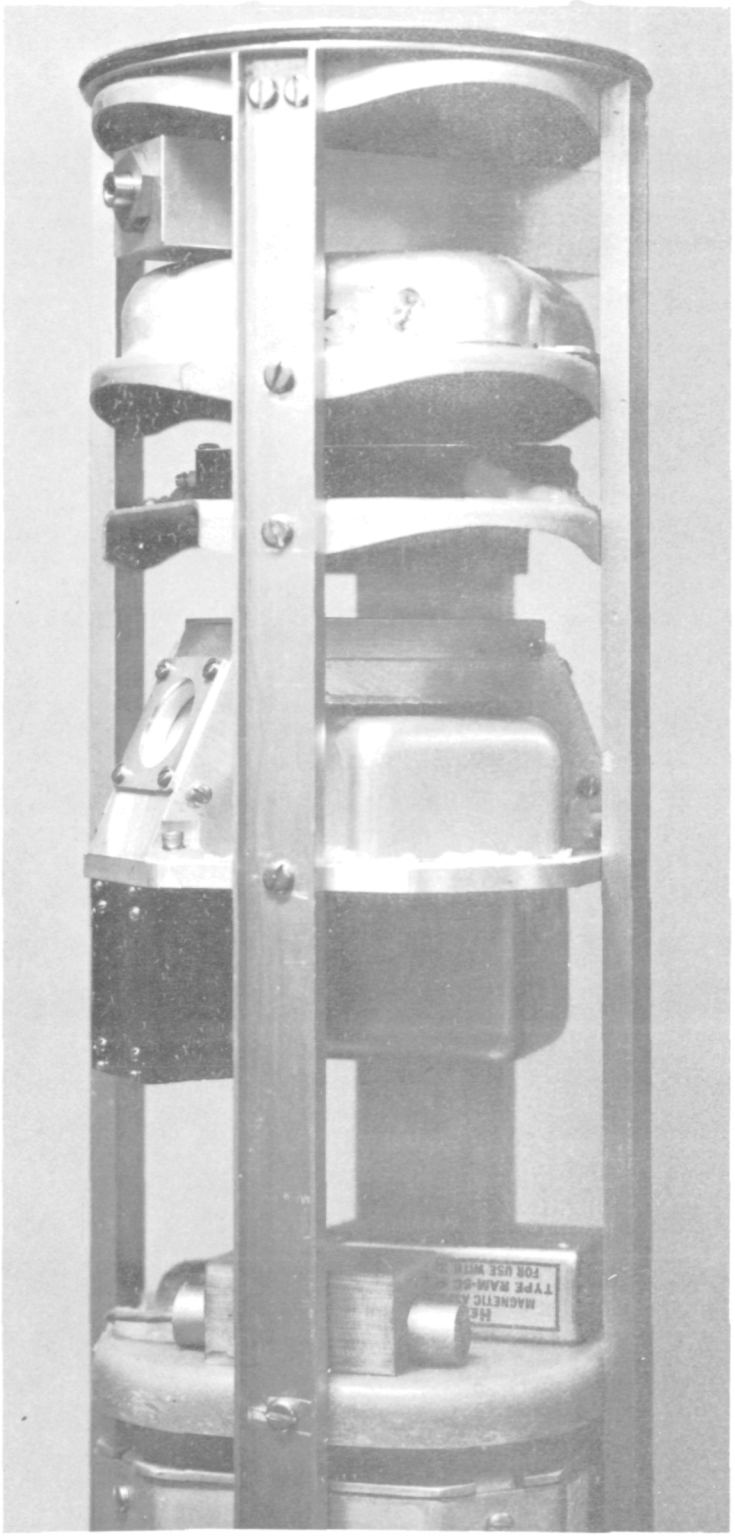

Figure 15. Section of Type A Mod 6 payload including solar radiation experiment and magnetic aspect sensor.

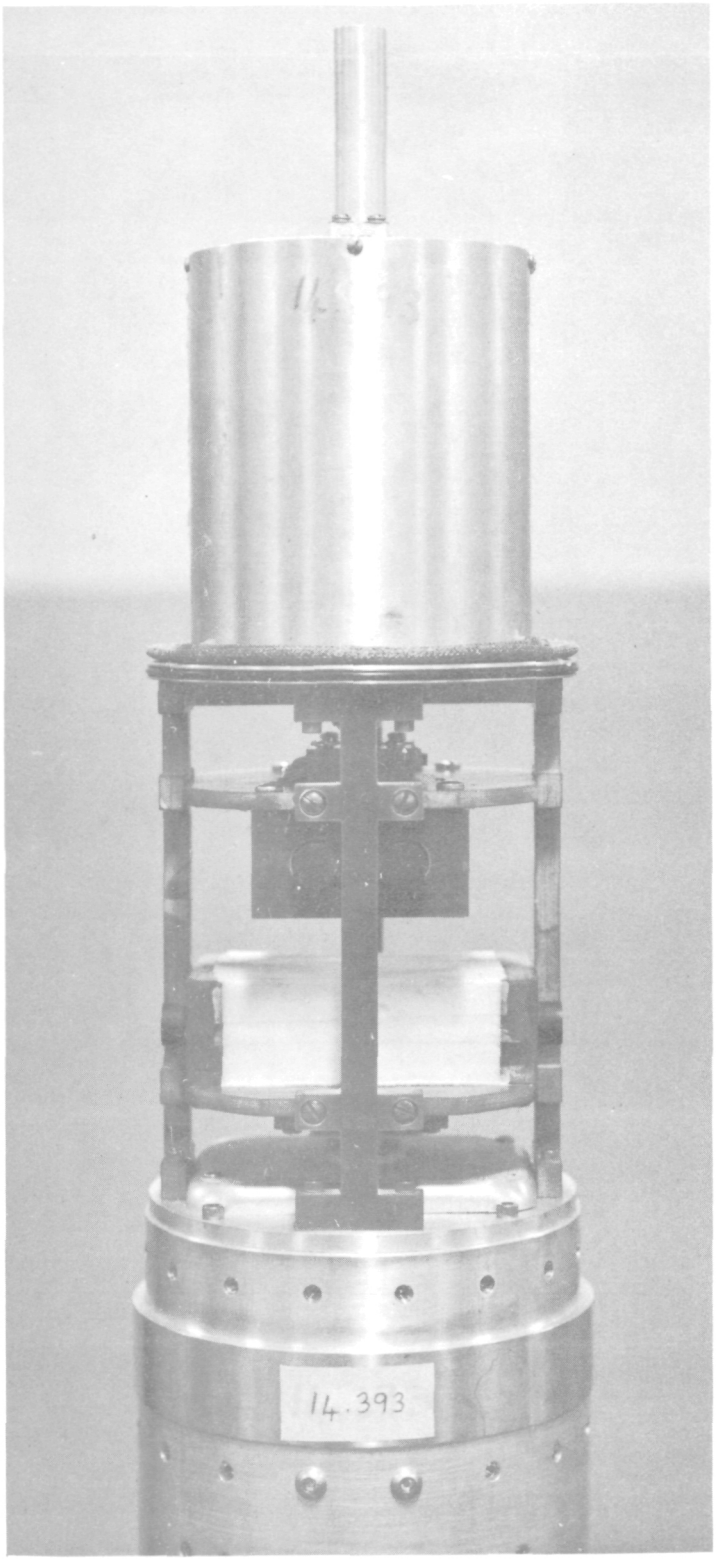

Figure 16. The antenna section for the two-frequency propagation experiment and the probe electronics package.

Figure 17. Payload, Type B Mod 4, with shell and nose cone removed. Flown on Nike Apache 14.394.

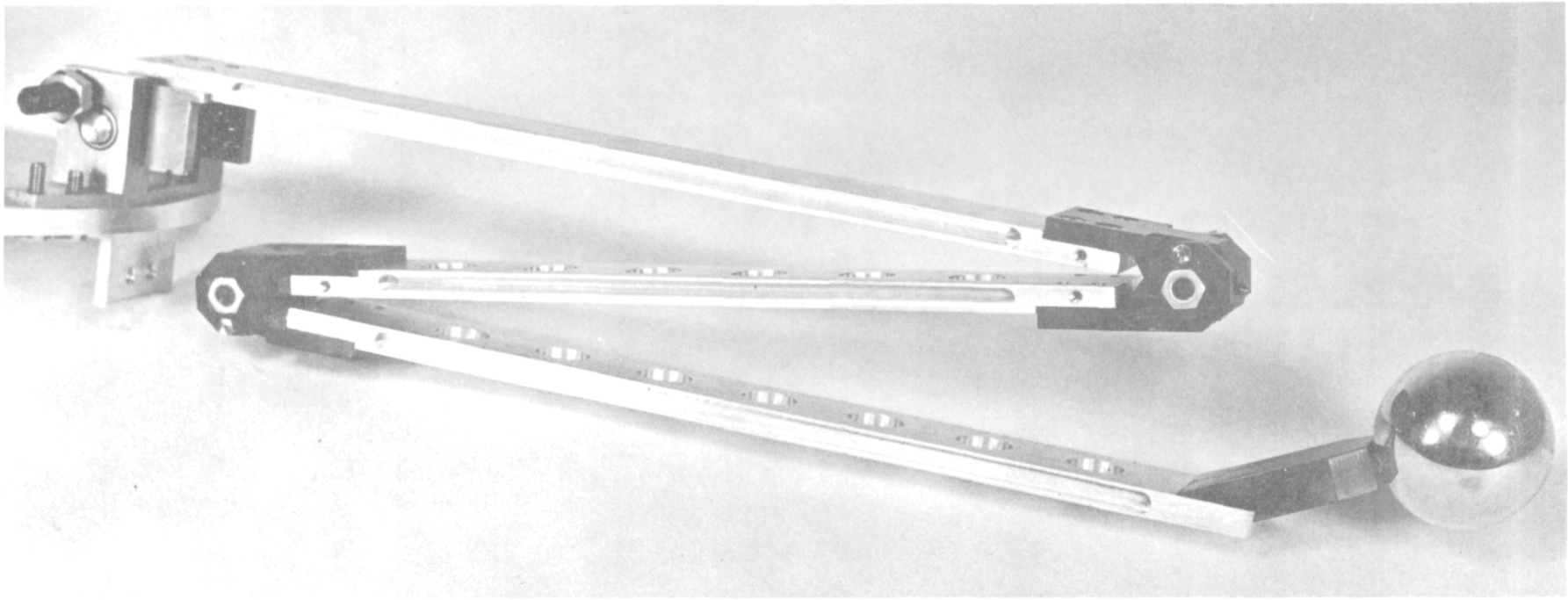

Figure 18. Construction of the boom, Type B payloads.

F. Payload Circuits

The control and interconnection circuits of the payload are illustrated in Figure 19. This is actually a Type A, Mod. 6 payload containing the two-frequency propagation experiment. The circuits for the other modifications of the three types of payloads are similar. The umbilical connector is at the left side of the drawing. Most connections are made directly to components on the control deck and thence, through connectors on the wiring channel to the various sub-assemblies in the sequence shown up to the propagation experiment and then the DC/Langmuir probe. Subsequent to this drawing, which shows the connections in detail for Nike Apache 14.393, baroswitches were added for redundency. The revision to the circuit is shown in Figure 20.

The baroswitches serve several functions:

(1) apply voltage to the power transfer relay; if this relay had become unlatched during the launch phase the payload would be switched on again at 40 kft;

(2) apply a voltage to energize the calibration relays in the experiments between 40 kft and 70 kft;

(3) arm the timer circuit at 70 kft;

(4) allow the determination of trajectory (in altitude only) if other methods of tracking should fail or give unreliable data.

The circuit of the electronic time delay is shown in Figure 21. Power is applied to the timer at an altitude of 70 kft by the baroswitches. After the appropriate elapsed time, about 13 seconds in the Type A payloads, the uni-junction transistor (Q1) conducts, causing the SCR (Q2) to turn on and energize the relay (K1). This applies voltage to the two bridges of the squib, a pressure cartridge (Holex 6200) in the door release mechanism. The timer monitor signal is combined with the solar aspect signal and telemetered on IRIG Channel 19.

The assignment of telemetry channels for the Type A, Mod. 5 and Mod. 6 and the Type B, Mod. 4 payloads is given in Table 7. Earlier modifications of the Type A payload were essentially the same as Mod. 5. There is some duration from this scheme for individual payloads of a given type and modification. A transmitter (Vector TRPT-250) rated at 0.25 watt was used for the earlier flights. A larger transmitter (Telemet 3008-A1), rated at 1 watt, was used in Type A, Mod. 5 and Mod. 6 and in Type B, Mod. 4.

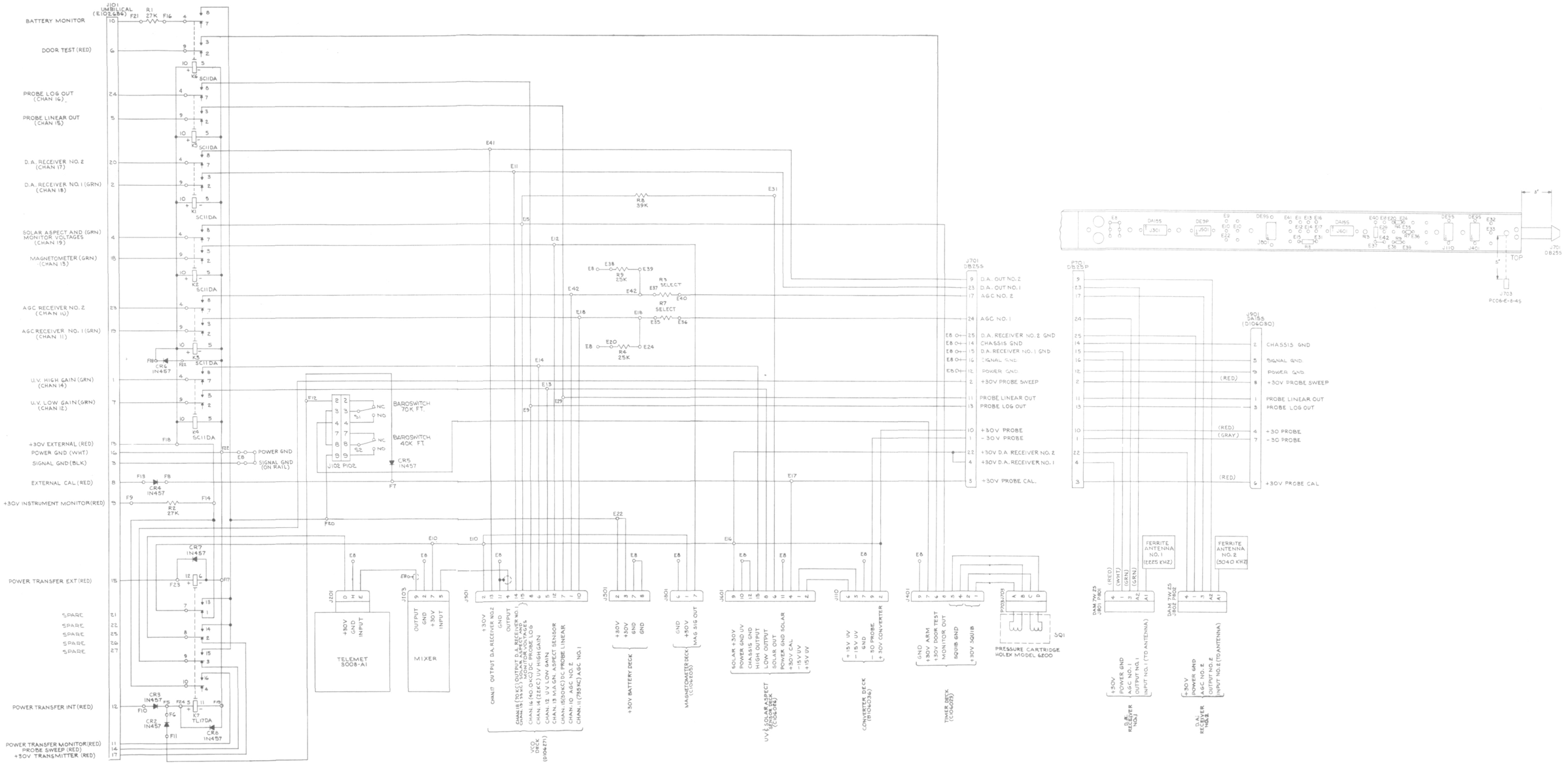

Figure 19. Interconnection wiring, Type A Mod 6 payload.

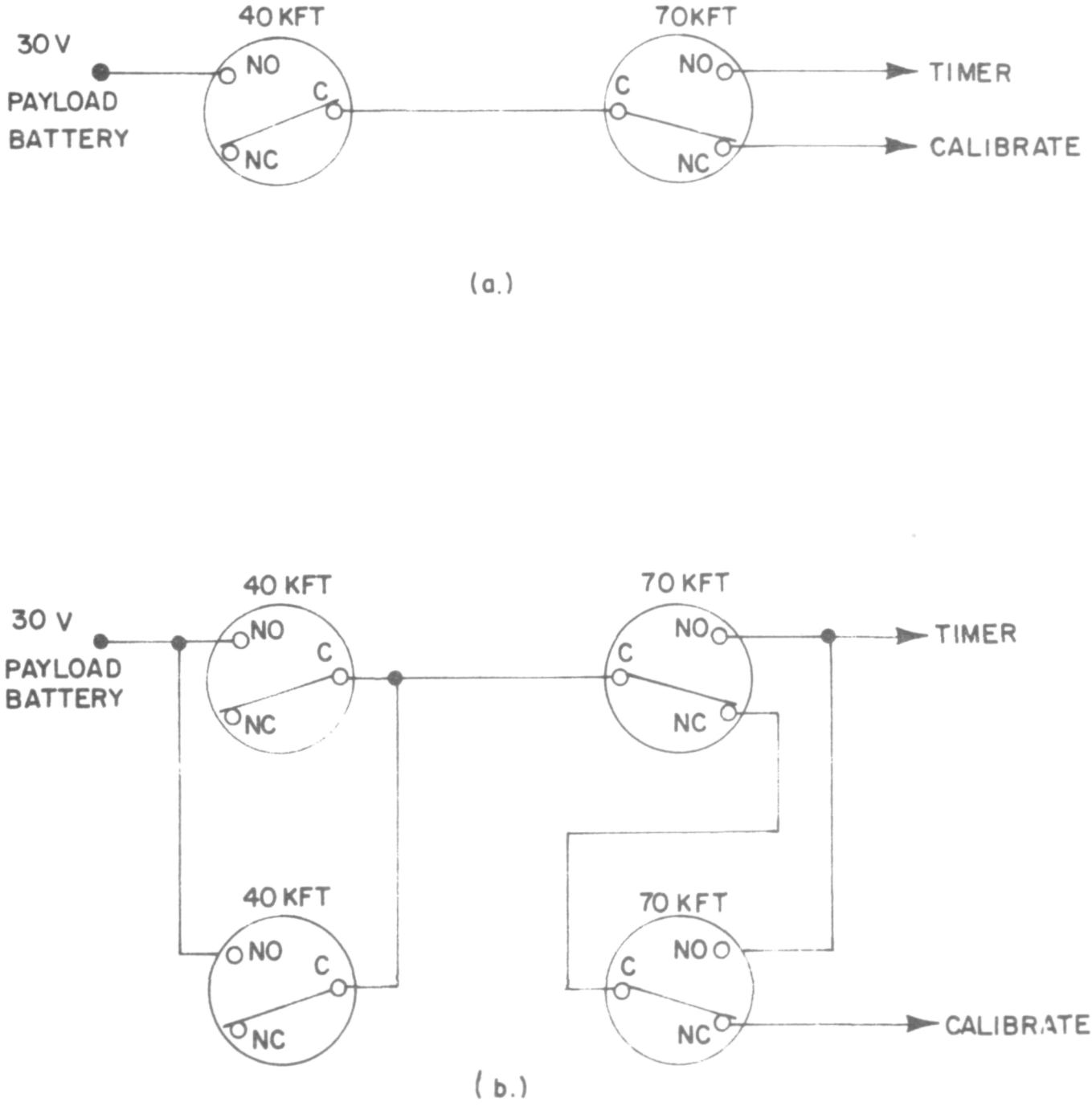

Figure 20. Baroswitch circuits, showing modification for increased reliability. Version (a) used in Nike Apache 14.393 and earlier flights; (b) used in Nike Apache 14.395 and subsequent flights.

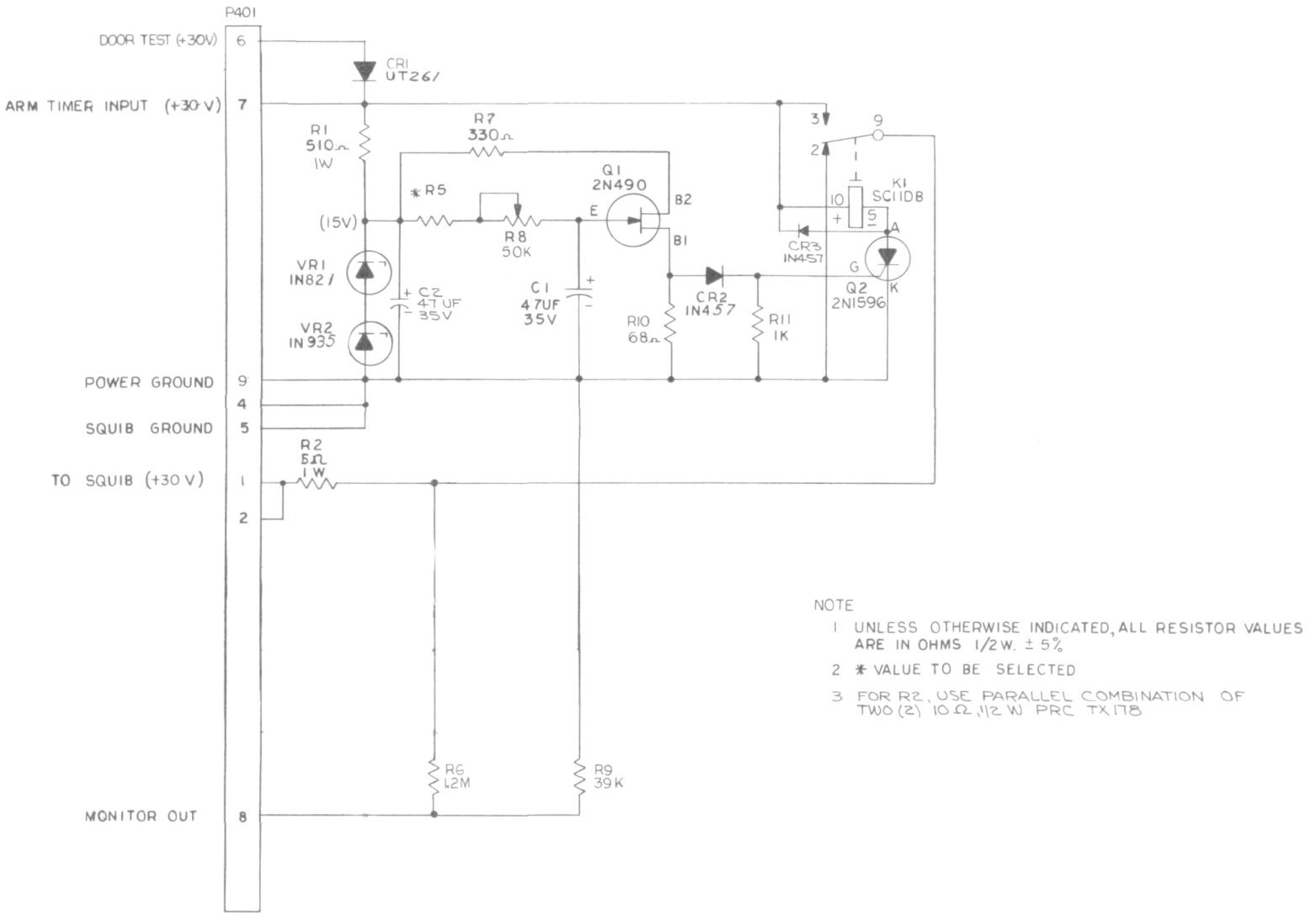

Figure 21. Electronic delay timer, Type A Mod 5 payload.

Table 7. Telemetry Channel Assignments

	Type A Mod. 5	Type A Mod. 6	Type B Mod. 4
Ch. 19	Solar Aspect and Monitor Voltage	Solar Aspect and Monitor Voltage	--------
Ch. 18	Receiver, Modulation	Receiver #1(2225 kHz), Modulation	Receiver(2225 kHz), Modulation
Ch. 17	Probe, Linear	Receiver #2(5040 kHz), Modulation	--------
Ch. 16	Probe, Log	Probe, Log	Probe, Log
Ch. 15	UV, High Gain	Probe, Linear	Probe, Linear
Ch. 14	UV, Low Gain	UV, High Gain	Ion Probe #1
Ch. 13	Magnetic Aspect	Magnetic Aspect	Magnetic Aspect
Ch. 12	----	UV, Low Gain	Ion Probe #2
Ch. 11	Receiver, AGC	Receiver #1, AGC	Receiver, AGC
Ch. 10	----	Receiver #2, AGC	Monitor, Voltage

IV. ELECTRON TEMPERATURE PROBE

A. Principle of Operation

The Langmuir probe technique is a powerful method of directly obtaining the electron energy distribution in a plasma. Druyvesteyn[1] showed that the energy distribution may be obtained from the current-voltage characteristic of the probe using the formula:

$$F(V_e) = \frac{1}{n}\frac{dn}{dV_e} = \frac{(8m)^{1/2}}{A\,e^{3/2}} V^{1/2} \frac{d^2 i}{dV^2} \qquad (1)$$

where V_e is the energy, n the number density, m the mass, and e the charge of the electrons, and A is the area, i the current, and V the potential (relative to plasma potential) of the probe. The second derivative of current with respect to voltage may be obtained by double differentiation of the plotted current-voltage characteristic. However, electronic methods have been developed in which this derivative is directly measured. This allows greater accuracy. The most successful of these techniques involve the superposition of one or two small amplitude ac signals onto the normal sweep voltage of the Langmuir probe.

In the method of Sloane and MacGregor[2] a small signal given by $E = A \sin pt$ is added to the probe potential V. If the current-voltage characteristic in the absence of the ac signal is represented by $i = f(V)$ then with the addition of the ac signal the current becomes:

$$i = f(V) + A\,f'(V) \sin pt + \frac{A^2}{4} f''(V)\,\{1 - \cos 2pt\} + \cdots \qquad (2)$$

where f' and f'' are the first and second derivatives of current with respect to voltage. The addition of the small ac signal results in a change in the average current given by

$$\Delta i = \frac{A^2}{4} f''(V)$$

provided that A is sufficiently small. Since A is known, a measurement of Δi leads immediately to $f''(V)$ and the energy distribution function. The frequency used in their experiments with gaseous discharges was 1000 Hz.

This method has been extended by Malyshev and Fedorov.[3] Instead of manually switching the ac signal, they vary the amplitude by sinusoidal modulation. The depth of modulation is 100 percent. In the notation of Sloane and MacGregor the small ac signal superimposed on the probe is $E = A\ (1 + \cos \omega t) \sin pt$ where $\omega \ll p$. The component of probe current at the modulation frequency $(\omega/2\pi)$ is selected in a narrow-band amplifier and detected, giving an output signal proportional to $f''(V)$. The frequencies used are not stated.

A similar method was developed independently by Boyd and Twiddy.[4] The carrier frequency (2000 Hz) is square-wave modulated (frequency 300 Hz) before being applied to the probe. The depth of modulation is 100 percent. The amplitude of the component of probe current at the modulation frequency is measured, as in the preceding method.

More recently Branner et al.[5] have returned to the unmodulated single frequency. It may be seen from Equation (2) that the amplitude of the component of probe current at the second harmonic of the impressed frequency is proportional to $f''(V)$. The frequency used is 1000 Hz. These authors discuss the three methods, i.e., sine-wave modulation, square-wave modulation and second harmonic, and find them to be essentially equivalent. This also includes complete circuit details.

The method of Boyd and Willmore[6] is the most recent of these techniques. It was developed specifically for rocket and satellite observations and has advantages when the energy distribution is Maxwellian, as is found to be the case in the ionosphere. The second derivative $f''(V)$ is not measured directly, but in the form $f''(V)/f'(V)$ which, for a Maxwellian distribution, is equal to e/kT. The first derivative is also measured and therefore, $f''(V)$ can be obtained, should it be desired to plot an energy distribution.

The principle of the method can be very simply stated. Two small amplitude ac signals are added to the probe voltage. The curvature of the current-voltage characteristic results in amplitude modulation of the higher frequency by the lower. The quantities measured are the depth of modulation, proportional to $f''(V)/f'(V)$, and the amplitude of the higher frequency, proportional to $f'(V)$. Note that in the methods of Malyshev and Federov and of Boyd and Twiddy, an amplitude-modulated signal is applied to the probe and the de-modulation is observed; in the method of Boyd and Willmore, two unmodulated signals are applied to the probe and the resulting inter-modulation is observed.

Consider a probe characteristic in the retarding potential region given by:

$$i = i_o \exp(V/V_e)$$

where i_o is the electron current to the probe at plasma potential

V is the potential of the probe relative to the plasma

V_e is the electron energy in voltage units (= kT/e).

The first and second differentials are given by:

$$f'(V) = \frac{di}{dV} = \frac{i_o}{V_e} \exp(V/V_e) = \frac{i}{V_e}$$

and

$$f''(V) = \frac{d^2i}{dV^2} = \frac{i_o}{V_e^2} \exp(V/V_e) = \frac{i}{V_e^2} \quad .$$

Thus, immediately, at any given potential in the retarding region

$$f''(V)/f'(V) = 1/V_e \quad .$$

Now consider an ac signal (the carrier), peak amplitude V_1, impressed on the sweep voltage. The peak amplitude of current variation at this frequency is from Equation (2)

$$i_1 = V_1 f'(V)$$

A second ac signal (the modulating signal), peak amplitude V_2, and frequency much lower than the carrier frequency is now added. The change in amplitude of i_1 at the peak of the modulating excursion is

$$\Delta i_1 = V_1 \{V_2 f''(V)\}$$

The depth of modulation of the carrier is thus

$$m = \Delta i_1/i_1 = V_2\{f''(V)/f'(V)\} = V_2/V_e$$

The simplified analysis given above assumes that V_1 and V_2 are small compared with V_e. An exact expression when V_2 is comparable with V_e is

$$m = 2I_1(V_2/V_e/I_o(V_2/V_e)$$

where I_o and I_1 are modified Bessel functions of the first kind of order zero and unity, respectively. Values of m for several values of V_2/V_e are given in Table 8.

TABLE 8

VALUES OF m AS A FUNCTION OF (V_2/V_e)

V_2/V_e	0	0.2	0.4	0.6	0.8	1.0
m	0.000	0.199	0.392	0.575	0.742	0.893

This indicates that a practical value of V_2 is equal to the smallest value of V_e that is anticipated. Although V_1 does not appear explicitly, its value should not be much greater than V_2 in order to keep the probe voltage excursion within the retarding region. In the instrument described by Bowen et al.[7] the carrier frequency is 3.2 kHz and its peak amplitude (V_1) is 54 mV; the modulating frequency is 500 Hz and its peak amplitude (V_2) is 35 mV. Thus, the instrument should be capable of measuring temperatures as low as 300°K.

The method of measuring the depth of modulation is shown in Figure 22. The two small ac signals are applied to the probe in series with the primary of a transformer. The waveforms shown in this figure were

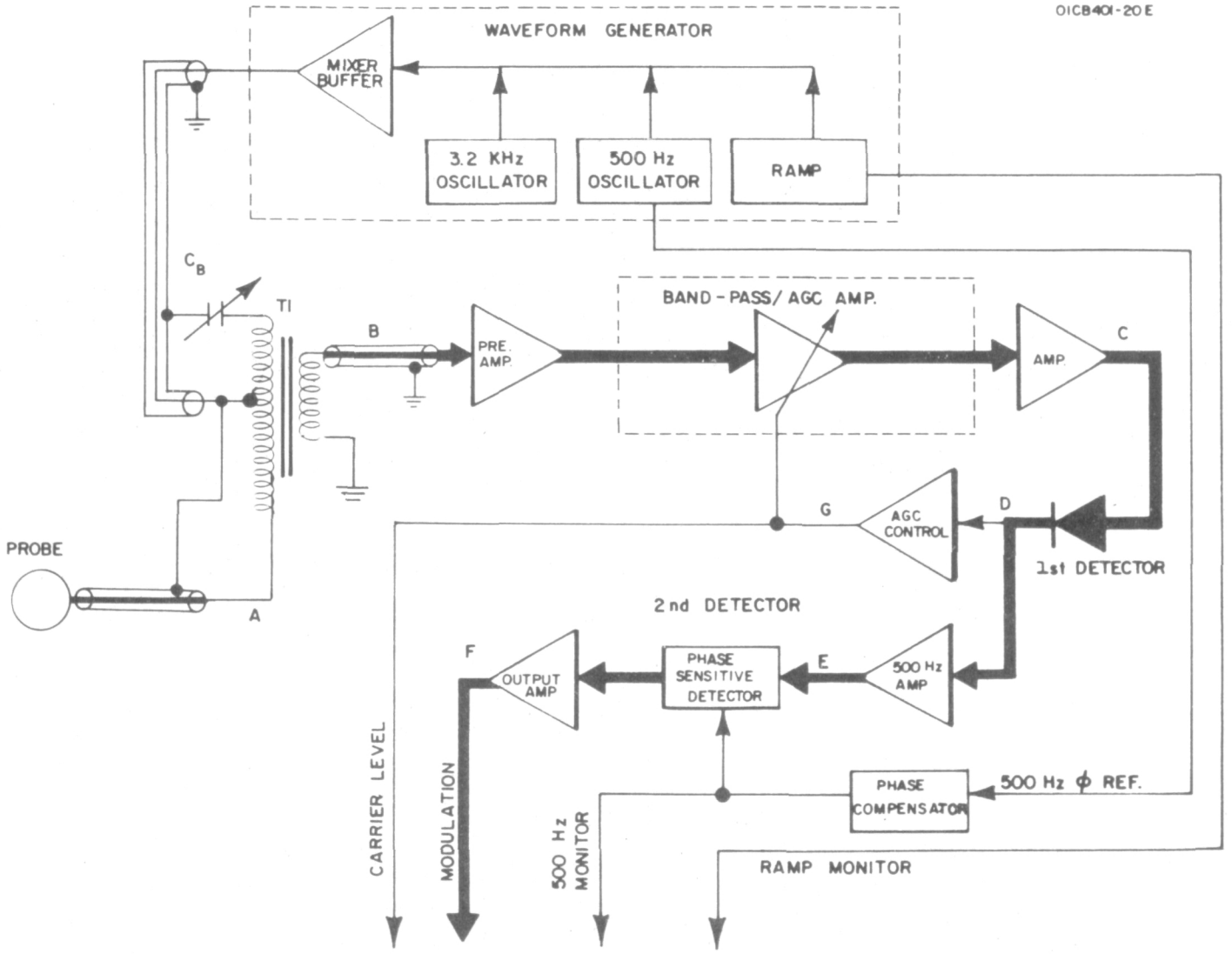

Figure 22. Electron temperature probe, simplified schematic.

obtained usin ac signals with frequencies of 500 Hz and 3.2 kHz and peak amplitudes of 15mV. The probe current-voltage characteristic is simulated by a resistor (1K) in series with a diode (1N483B). The horizontal scale is 1 ms/cm (on the oscilloscope screen) and the vertical deflections as follows: A, 20 mV/cm; B, about 0.1 mV/cm; C, 0.5V/cm; D, 0.2V/cm; E, 0.1V/cm; and F, 0.2V/cm.

The appearance of the signal on the probe as observed at point A is shown in Figure 23. The resulting variation in probe current as observed at point B contains unwanted components principally at 500 Hz and 1.0 kHz. These are removed in the first amplifier which has a pass-band 2.7 to 3.7 kHz. The signal at the output is seen at point C. This signal is detected and the modulating frequency appears at point D. The average level of carrier signal applied to the first detector is held constant by applying automatic gain control (AGC) to the band-pass amplifier. The amplitude of the 500 Hz signal developed at D is thus, proportional to the depth of modulation.

After further amplification the signal, seen at point E, is detected in a phase-sensitive detector, the reference signal being obtained from the 500 Hz oscillator. The phase-sensitive detector also allows linear detection at small signal levels and has the further advantage of discrimination against unwanted signals. While the probe is in the retarding potential region for electrons, the output of the instrument, at point F, is thus an analog voltage which is inversely proportional to electron temperature.

The probe voltage is swept from -2.7 to +3.5V with a period of 55 sec. in the instrument of Boyd and Willmore. This serves two purposes: (1) it allows a complete energy distribution to be recorded, and (2) it allows the vehicle potential to be determined. By omitting the sweep and assuming that the energy distribution is Maxwellian, it appears to be possible to obtain a continuous temperature measurement.

In the instrument which has been developed, the probe electrode will be insulated from the payload and allowed to attain floating potential. This is the potential, in the electron retarding region, at which the positive ion current equals the electron current. Experience on previous rocket flights with a simple Langmuir probe shows that this is a suitable potential at which to make the electron temperature measurement. The only change from the instrument shown in Figure 22 is the insertion of a low-leakage capacitor at the point A, between the transformer and the probe electrode. The ramp generator is retained to provide a comparison of the floating-potential and swept-potential modes and to give a method of in-flight calibration of the instrument. The input circuit of the new instrument is shown in Figure 24. The calibration uses a series combination of silicon diode and

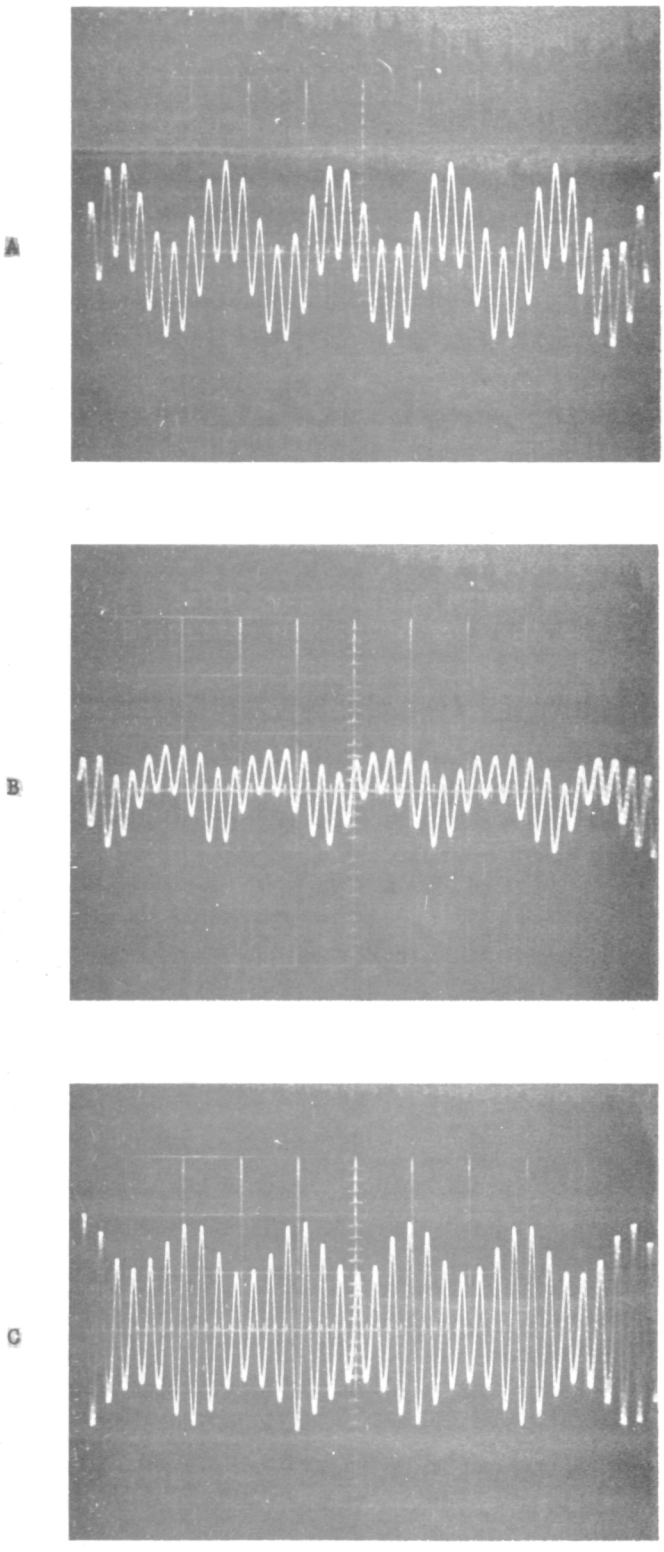

Figure 23. Electron temperature probe waveforms, recorded at points indicated in Figure 22.

D

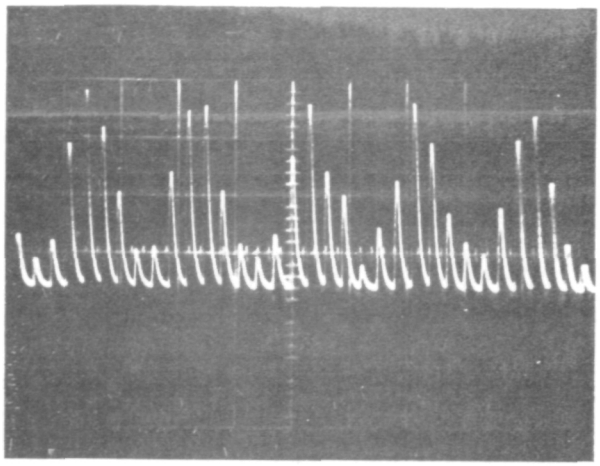

E

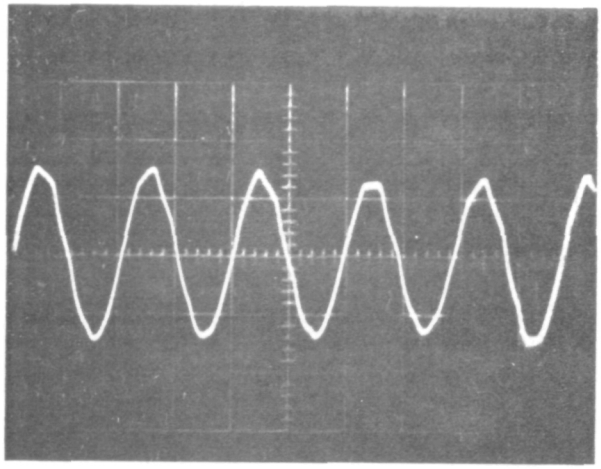

F

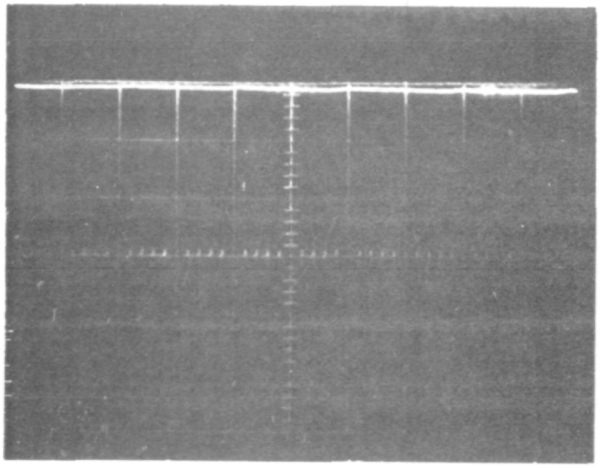

Figure 23 (continued)

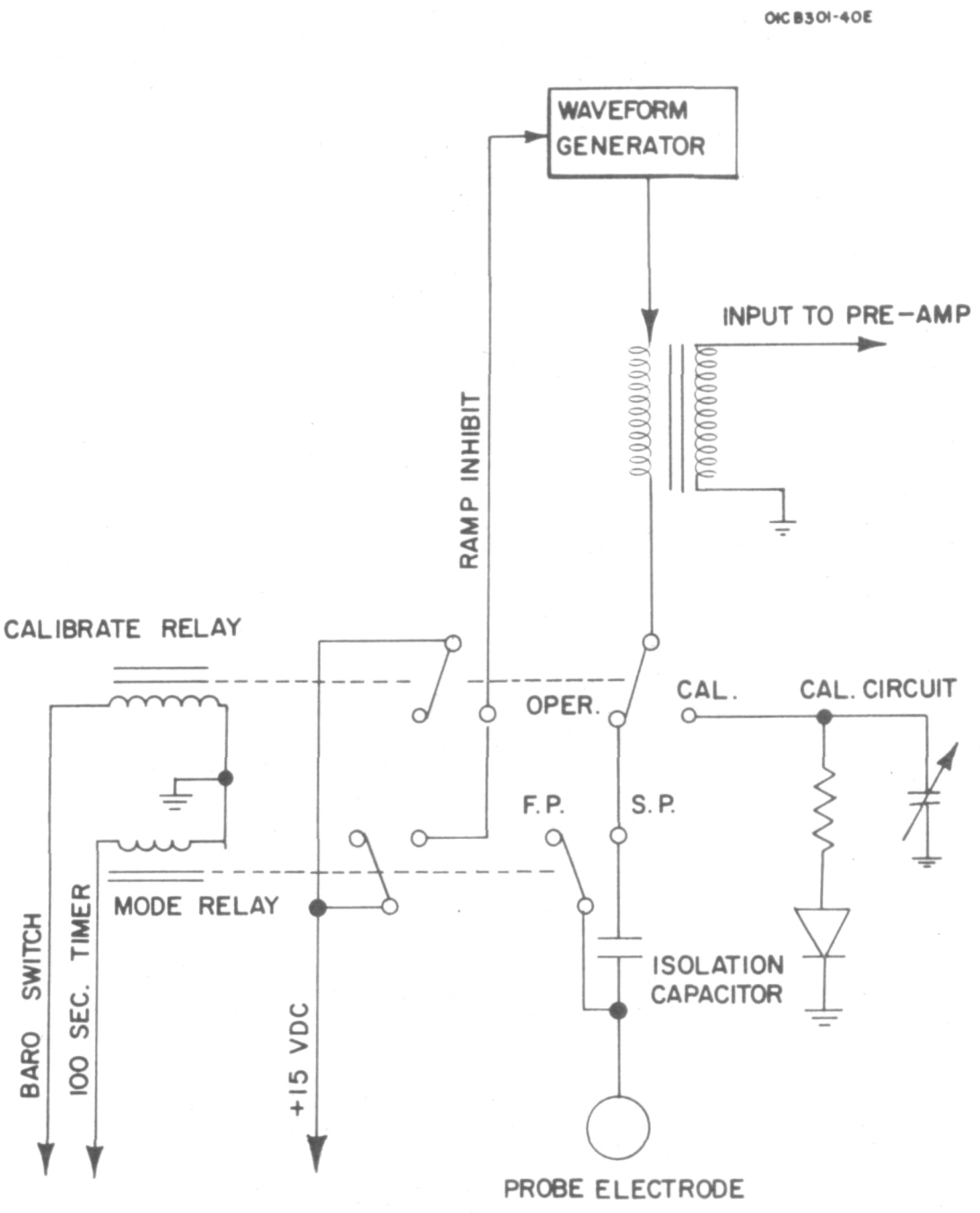

Figure 24. Method of mode-switching and in-flight calibration.

resistor: this gives a good approximation to a temperature of about $300^{o}K$.

The principal difficulties of the circuit design are attributed to: (1) the low level of the signal at the input to the first amplifier, and (2) the relative closeness of the two frequencies.

B. Instrument Operation

The waveform generator produces three outputs:

(1) A 500 Hz sinusoidal signal at 25 mV amplitude

(2) A 3.2 kHz sinusoidal signal at 50 mV amplitude

(3) A linear ramp from -0.5 VDC to +2.5 VDC with a three second sweep period.

The three outputs are combined in the adder-buffer stage, Figure 22, and applied to the probe in series with the primary of the input transformer. Since the probe voltage-current characteristic is non-linear, the probe current contains components at 500 Hz (f_1), 3.2 kHz (f_2) and a cross-modulated term at $f_2 \pm f_1$. The probe contains components at frequencies of $Mf_2 \pm Nf_1$. It is the amplitude of the cross modulated terms, $f_2 \pm f_1$, directly proportional to $f''(V)$, that the system must measure. $f''(V)$ is not measured directly, but in the form $f''(V)/f'(V)$ proportional to depth of modulation. f_2 (carrier level) proportional to $f'(V)$ is also measured so $f''(V)$ can be determined.

The composite probe signal at point B is amplified by the preamplifier and fed to the bandpass/AGC amplifier. Here, $f_2 \pm f_1$ are selected and the modulating frequency f_1 and its second harmonic are rejected. The output signal is observed at point C. This signal is detected at the first detector as seen at point D. Here, f_2 (carrier level) is filtered as an AGC voltage to control the gain of the bandpass/AGC amplifier. This assures the average carrier level output to the first detector to be nearly constant over an input current range of nearly four orders of magnitude. Also, the amplitude of the demodulated 500 Hz (f_1) signal developed at D is proportional to $f''(V)/f'(V)$ (depth of modulation).

The AGC voltage proportional to $f'(V)$ is telemetered and is a measure, on an approximately logarithmic scale, of the probe current over the range 2×10^{-10} to 10^{-6} amps rms.

The 500 Hz demodulated signal at D is now applied to a tuned 500 Hz selective amplifier. The output of this amplifier at E is fed to the second detector. This is a phase sensitive detector requiring a 500 Hz 6-volt peak-to-peak reference signal from the 500 Hz oscillator for operation. The detector gives an analog voltage output at F proportional to signal input at E. The output at F is, therefore, a voltage inversely proportional to electron temperature. As the input signal changes phase by π, the output changes polarity allowing the sign of $f''(V)$ to be determined. The detector also serves to discriminate against unwanted signals at other frequencies.

The signals are telemetered as follows:

(1) Electron temperature (modulation depth) on IRIG Channel 15.

(2) AGC voltage (carrier level) commutated at 37.5 samples/sec on IRIG Channel 12.

(3) Ramp voltage commutated at 2.5 samples/sec on IRIG Channel 12.

(4) 500 Hz oscillator peak voltage commutated at 2.5 samples/sec on IRIG Channel 12.

C. Circuit Details

The complete circuit is shown in Figure 25.

Waveform Generator. - The waveform generator consists of a 500 Hz sinusoidal oscillator, a kHz sinusoidal oscillator and a linear ramp generator. Both oscillators are the Wien Bridge type utilizing good frequency amplitude stability and low-harmonic content. Harmonic content is less than 1 percent and frequency stability less than 0.5 percent from $0^{\circ}F$ to $110^{\circ}F$. The 500 Hz oscillator has two outputs at 25 mV peak and 3 V peak $\pm$ 1 percent. The 3.2 kHz oscillator output is 50 mV peak $\pm$ 1 percent.

Amplitude stability is a critical requirement, especially for the 500 Hz oscillator. It is accomplished by peak-detecting the oscillator output and using this voltage to control the dynamic drain-to-source resistance (R_{DS}) of a 2N2608 Field Effect Transistor (FET) in the negative feedback loop of the oscillator. As the drain-to-source voltage (V_{DS}) of FET approaches zero, the drain-to-source resistance (R_{DS}) is very nearly a linear function of the gate-to-source voltage (V_{GS}) as long as V_{GS} is below the pinch-off voltage. For high values of V_{GS}, approaching pinch-off, R_{DS} becomes very nonlinear, due to departure of the FET transfer characteristic from square-law behavior at low drain currents.

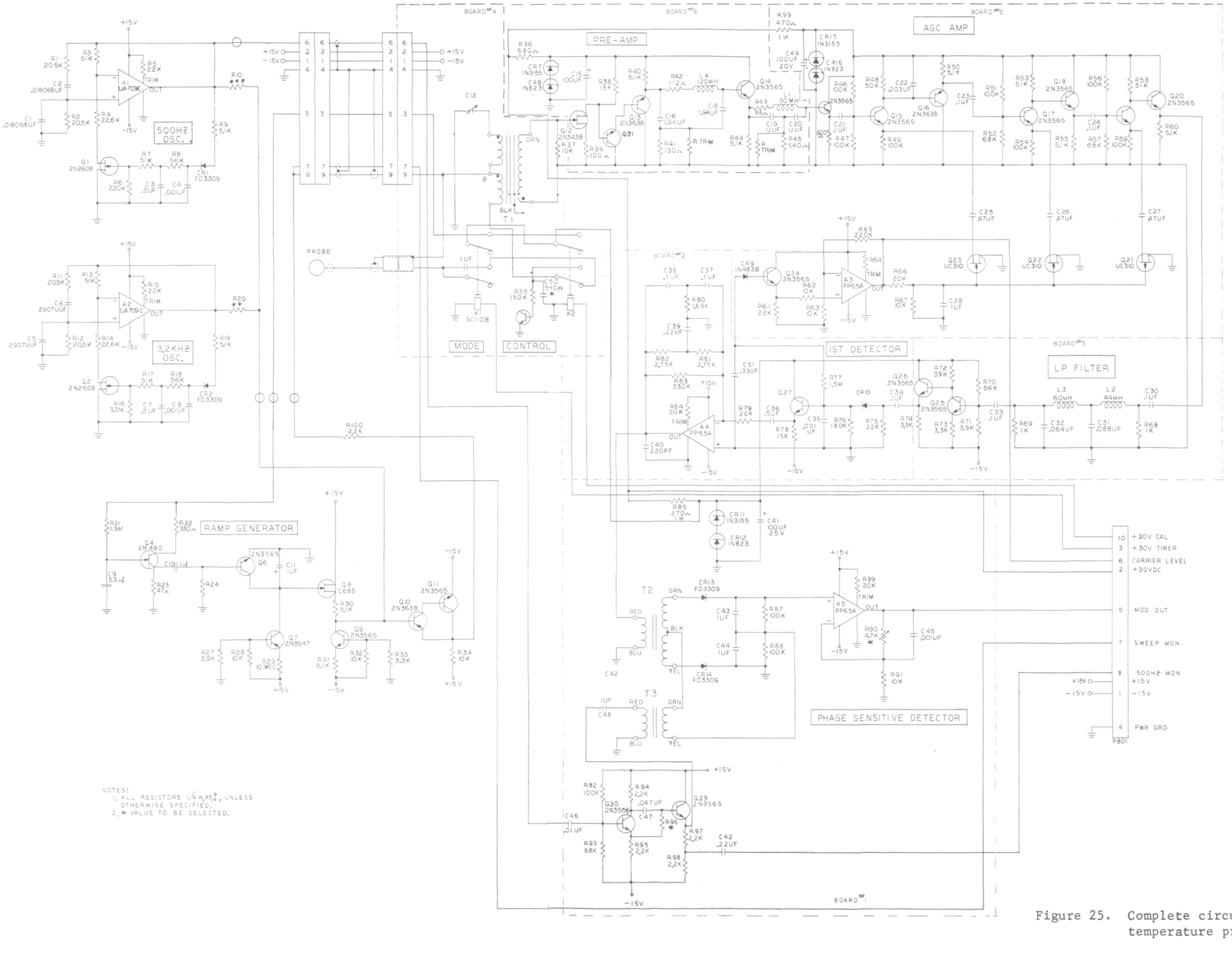

NOTES:
1. ALL RESISTORS 1/4 W, ±5%, UNLESS OTHERWISE SPECIFIED.
2. * VALUE TO BE SELECTED.

Figure 25. Complete circuit of the electron temperature probe.

The linear ramp generator is a constant-current RC charging circuit reset by a free running (a stable) multi-vibrator every three seconds $\pm$ 0.2 seconds. The ramp voltage is from -0.5 V to +2.5V $\pm$ 5 percent. The reset time is 1.5 μ sec. $\pm$ 0.1 percent.

Input Circuit. - The input transformer (James Electronics Inc. No. 8125) has high electromagnetic and electrostatic shielding with 140 db of common mode rejection. The maximum interwinding capacitance is 5×10^{-7} pf and the maximum impedance unbalance is 0.1 percent. A turns ratio of 1.1 was selected so the input impedance of the primary is controlled by the load on the secondary. This also makes it convenient for determining signal current levels. The transformer frequency response was determined for various probe impedances of 5×10^4 to 10^7 ohms (expected dynamic range of impedance in the ionosphere) using secondary loads of 5×10^3 ohms to 10^4 ohms. Optimum response from 2.7 kHz to 3.7 kHz was obtained for 10^4 ohms on the secondary with an output deviation versus frequency of less than 1 db.

One side of the balanced dual primary of the transformer is the transfer winding in series with the probe. The other side is connected 180^o out-of-phase through a variable capacitor C_B to ground. C_B neutralizes the effects of the finite capacitance of the probe which would indicate a voltage error in the carrier level output. C_B can balance out the effects of this signal to less than one micro-volt at the input. The effect of cable capacitance is reduced by using low capacitance, low noise cable and driving the shield to the probe.

The mode select circuit determines the in-flight mode of operation by selection of relays by 40 kft and 70 kft baroswitches and an electronic timer. The three modes of operation are:

(1) Floating potential (F.P.) mode.
(2) Swept potential (S.P.) mode.
(3) Calibrate mode.

In the floating potential mode a 1 μf low-leakage capacitor is connected in series with the probe and a relay holds the ramp generator off. In the swept potential mode a 100-second timer selects a relay to short the 1 μf capacitor and turn on the ramp generator. In the calibrate mode the baroswitches activate the calibrate relay which connects a series resistor diode combination selected for system calibration.

Input Amplifiers. - The pre-amplifier is a low noise common source FET amplifier with a gain of 20. The output is buffered with an emitter follower for light loading of the amplifier.

The major effort in circuit development was concerned with the narrow band amplifier and AGC system. The result is a cascaded three-stage common-emitter amplifier with input and output filtering to shape the passband of interest. Each stage is suitably buffered for light loading.

Variable gain is accomplished by detecting and filtering the 3.2 kHz carrier output at the first detector and using this as an AGC voltage to control the gain of each stage. This AGC voltage, proportional to carrier level, becomes the gate to source voltage (V_{GS}) of three UC310 FETs A.C. coupled across each emitter resistor in each stage of the amplifier. The drain to source resistance (R_{DS}) of each FET is almost linearly proportional to carrier level so long as the AGC voltage (V_{GS}) is below the pinch-off voltage (V_P) of the FET. This is similar to its use for the Wien bridge oscillators.

The amplifier voltage gain, therefore, is approximately inversely proportional to carrier level. An approximate expression for the three stage gain is:

$$G = \left[\left(-g_m\left(\frac{V_{AGC}}{V_P} - 1\right) + \frac{1}{R_e}\right) R_C\right]^3$$

where:

g_m = pinch-off transconductance

V_P = pinch-off voltage

R_C = amplifier collector resistor

R_e = amplifier emitter resistor

The expression assumes the FET to be a square law device. This is true for gate-to-source voltages below V_P. The gain departs from linearity as the AGC voltage approaches V_P, due to departure of the FET transfer characteristic from square law; refer to Figure 26 and Figure 27. An amplifier dynamic range of 80 db was obtained without appreciable distortion.

The input to the variable gain amplifier consists of two bridged-T notch filters at 1 kHz and 500 Hz. These filters are designed for a 20 db minimum attenuation of the 500 Hz modulating signal and its second harmonic. They are also predominant in shaping the lower passband of the amplifier. A plot of the characteristics of these two filters is shown in Figure 28.

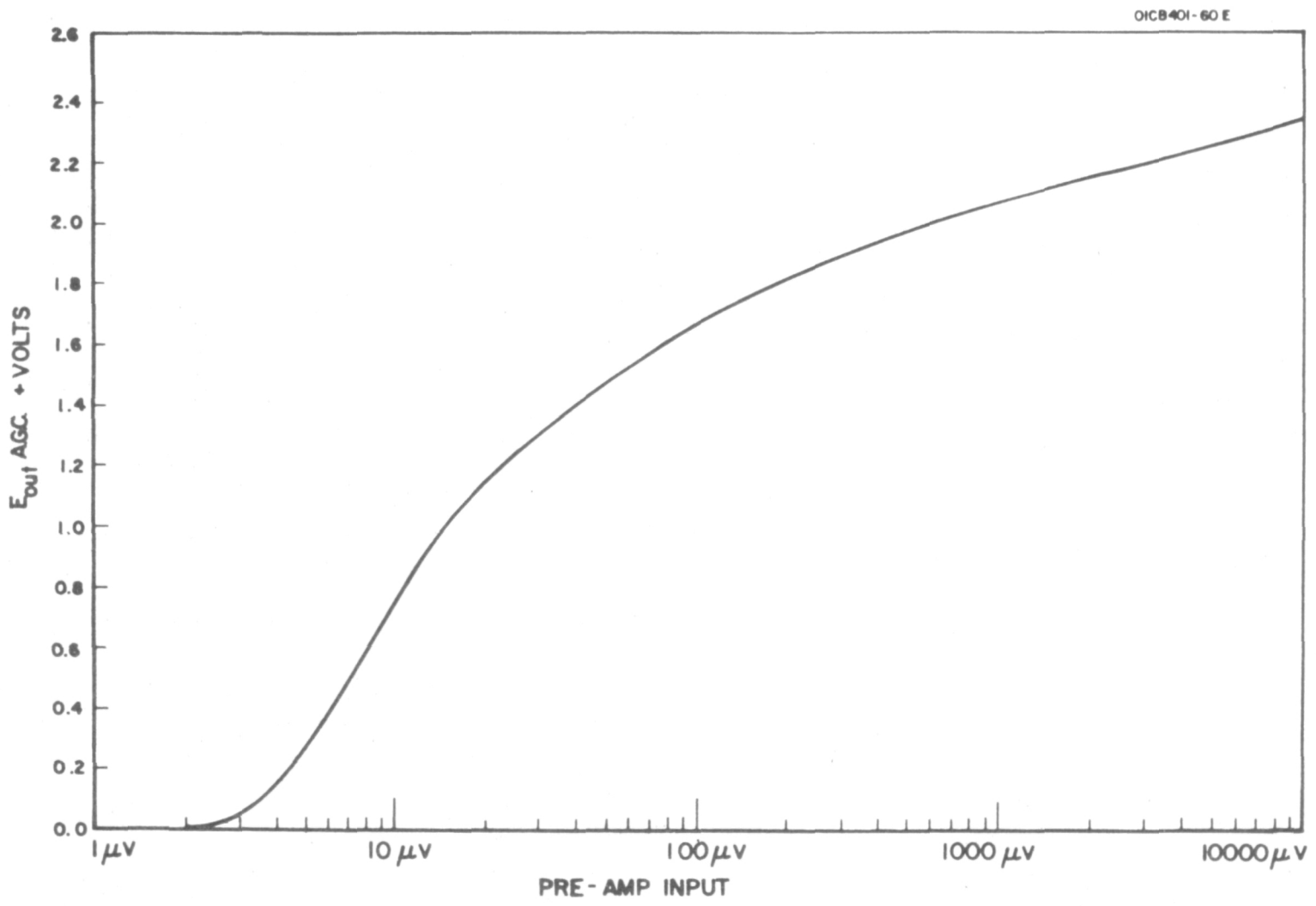

Figure 26. AGC amplifier; input versus output volts.

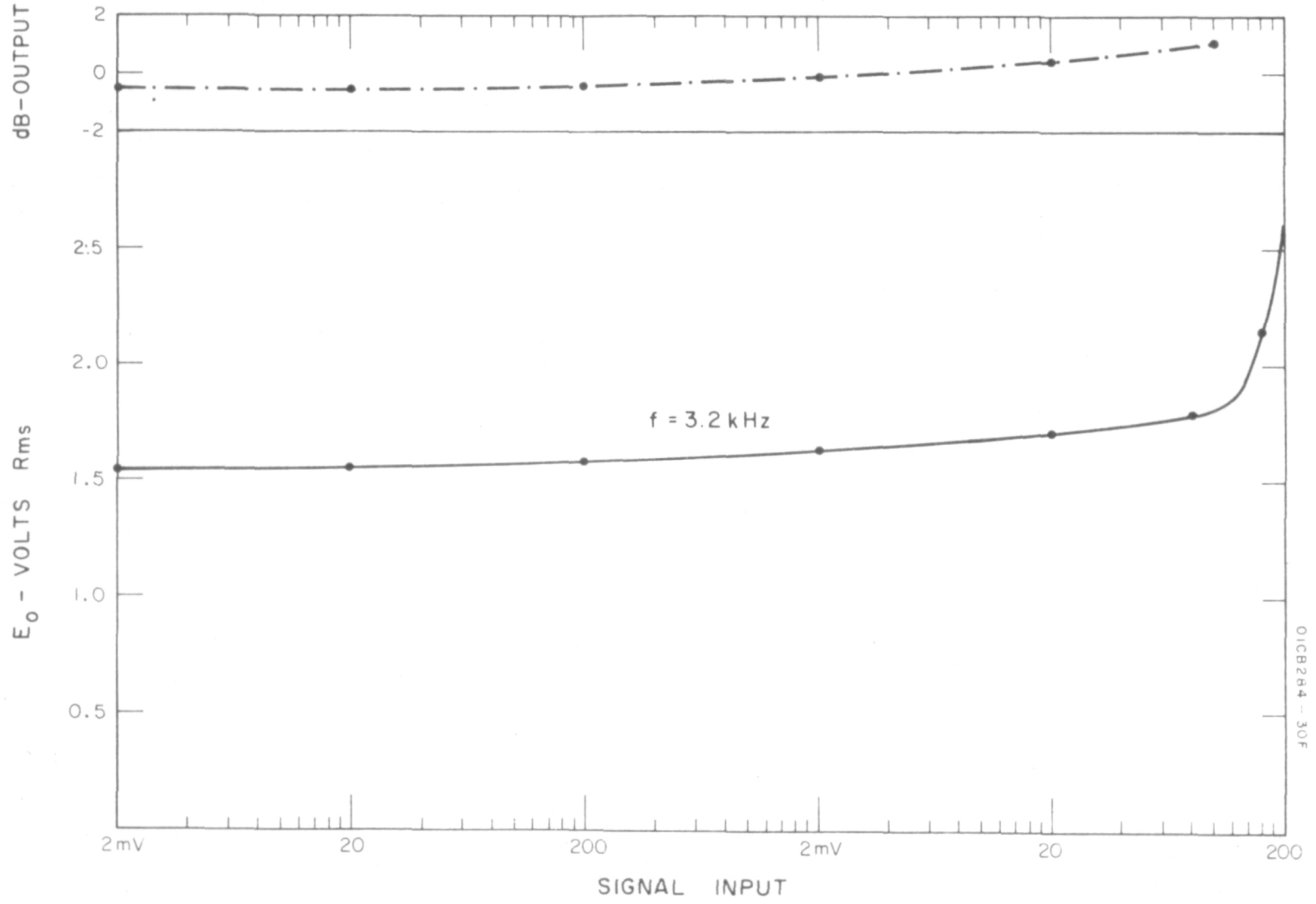

Figure 27. AGC amplifier characteristic.

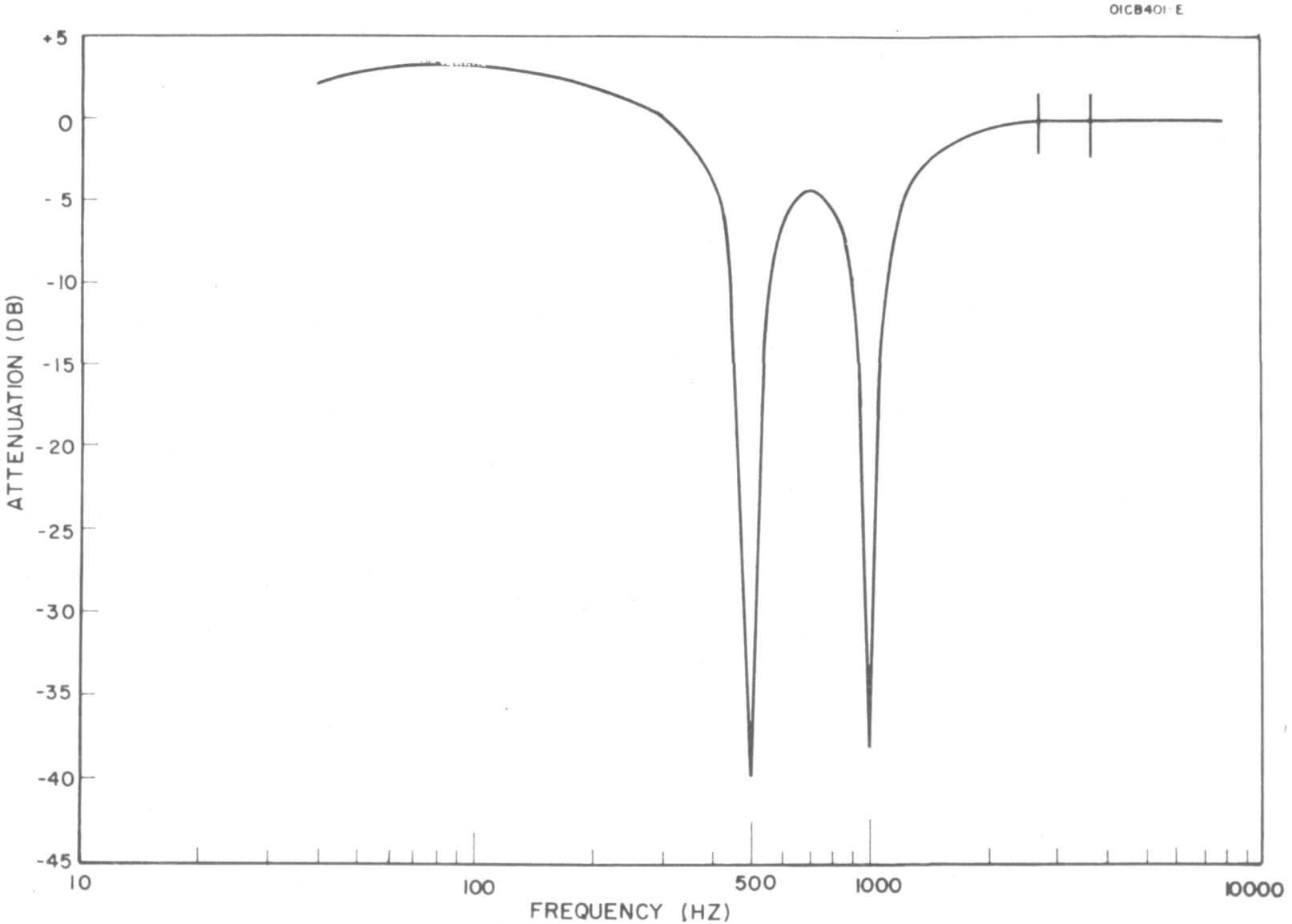

Figure 28. Input bridge-T filter response. 3.2 kHz is 0db reference.

The amplifier output filter is a four-pole Butterworth lower pass filter. It is designed to shape the upper passband gives maximum attenuation of frequencies above $f_2 + f_1$ with the second harmonic of the 3.2 kHz carrier down 20 db. The amplifier response is shown in Figure 29. The bandpass-AGC amplifier is designed to meet the following specifications:

Input Signal Range - 2 μ volts rms to 20 mV rms

Output into 1st detector - 1.5 volts rms ± 1 db over input dynamic range

Frequency Response - (1) Passband (2.7 to 3.7 kHz) flat to ± 0.5 db

(2) Frequencies 500 Hz, 1 kHz and 6.4 kHz to be 20 db below passband.

500 Hz Selective Amplifier. - This amplifier consists of a Philbrick PP65 operational amplifier with a parallel-T filter inserted in the negative feedback loop. The Q of the filter is low to keep the phase shift small, within the frequency stability limits of the 500 Hz oscillator, while retaining good selectivity and S/N ratio of the 500 Hz signal. The amplifier gain gives a 5 V p-p output for a modulation depth of 0.8 at the 1st detector.

Second Detector. - This circuit consists of a simple diode push-pull detector with a Philbrick PP65 operational amplifier output and a phase compensation circuit. The diode detector serves as an amplitude and phase detector. The dual transfor input requires two inputs for operation:

(1) The 500 Hz signal input proportional to depth of modulation.

(2) A 500 Hz reference signal at 6.0 V peak-to-peak constant amplitude and in-phase with the signal input.

The output amplitude is linearly proportional to the signal input, provided the reference signal is of greater amplitude than the expected maximum input signal level. The circuit offers improved signal-to-noise discrimination and, to the extent that the circuit is balanced, there is no response to even order harmonics.

The phase compensation circuit serves to compensate for phase shifts in the 500 Hz signal between the oscillator and phase detector. It gives a variable phase shift of 160° ± 5 percent while retaining a

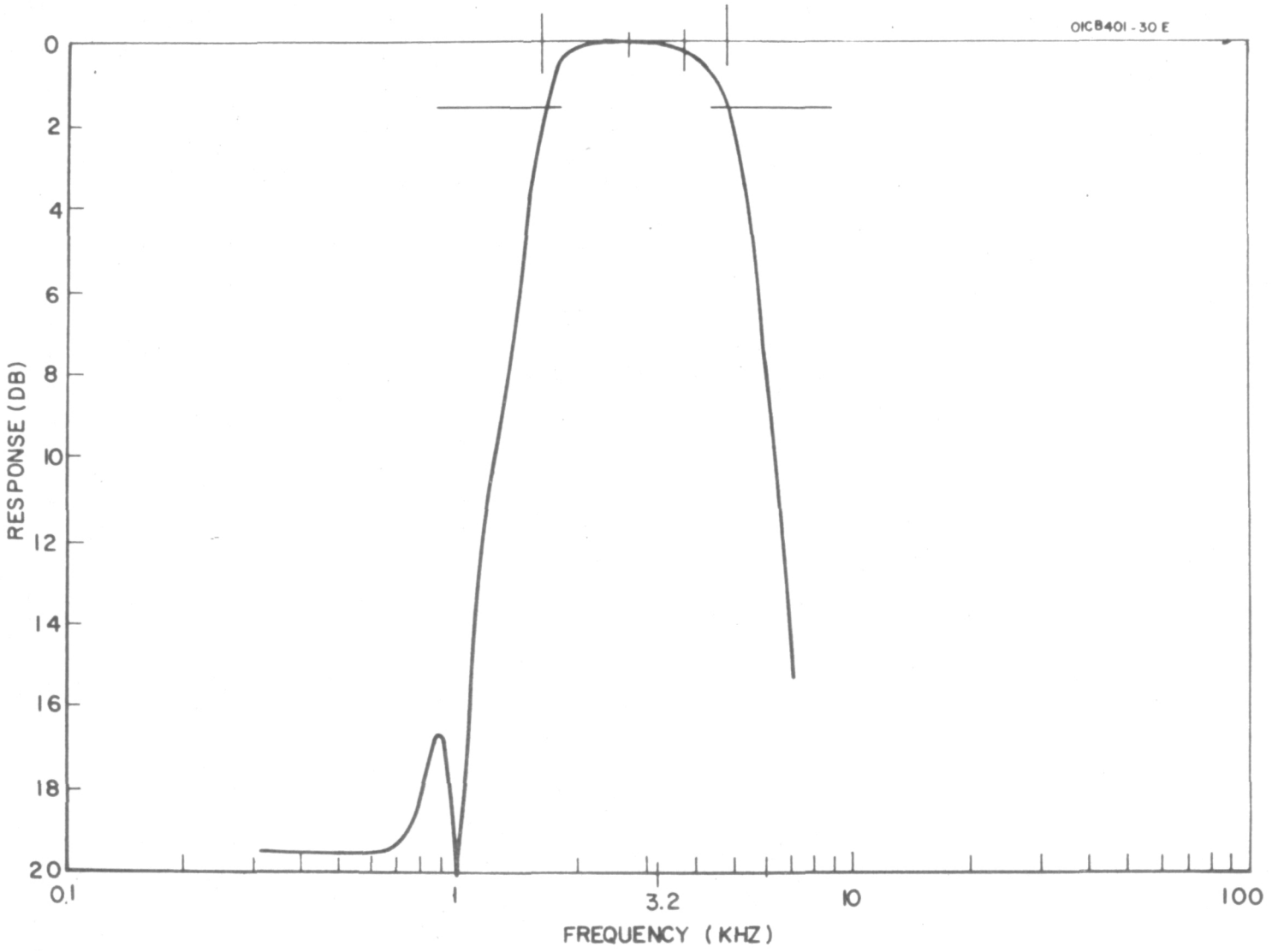

Figure 29. Bandpass - AGC amplifier response.

gain of 1 $\pm$ 5 percent. The circuit consists of a transistor amplifier with a gain of unity and a selected resistor in an RC network to give the phase compensation required.

D. Performance

The response of the instruments during calibration is shown in Figure 30. The horizontal scale is 200 msec/cm (on the oscilloscope screen). The upper waveform is the output of the phase sensitive detector observed at F, Figure 22. The corresponding variation in the AGC signal, observed at G, Figure 22, is shown in the lower waveform. The signals show a relatively narrow peak rather than the constant level that would be expected from an ideal (exponential) variation of probe current with voltage. As the ramp begins, the current-voltage characteristics is linear (representing positive-ion current collection). Then as the electron current becomes larger, the curve gradually changes to the exponential form: the increasing currative producing the increase in modulation index. When the positive-ion current becomes negligible, the modulation index is constant. Further, increase in potential of the probe moves it into the accellerating region (for electrons) and the modulation index decreases as the current-voltage characteristic becomes less curved. The calibration arrangement used a combination of resistors and a diode and the current-voltage relation becomes essentially linear at the end of the sweep causing the modulation index to fall to zero.

The inverse relationship between output voltage and electron temperature, expressed in voltage units (1 volt = 11,610^{o}K), is shown in Figure 31.

(a)

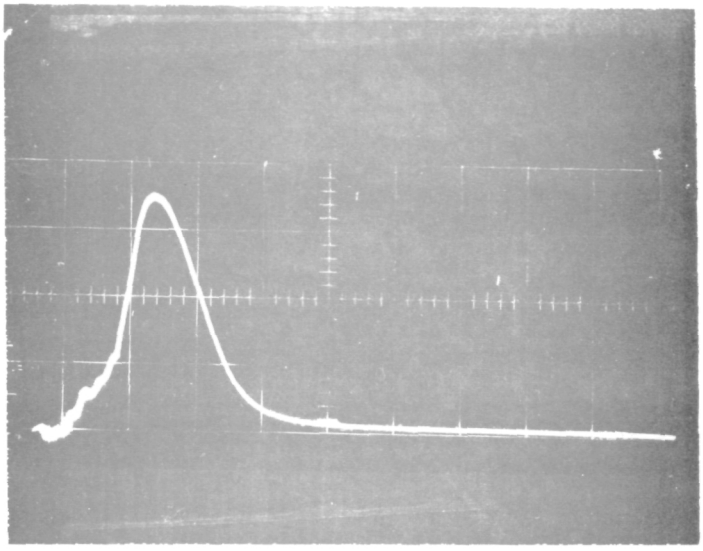

(b)

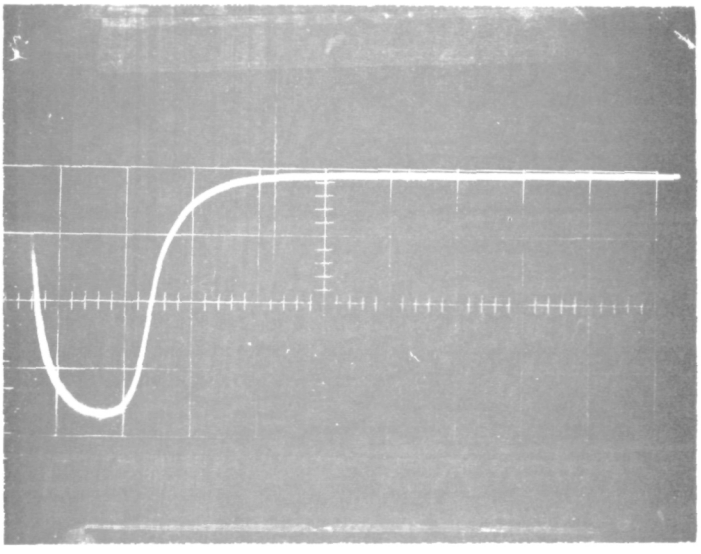

Figure 30. Response of the electron temperature probe during calibration: (a) output of second detector and (b) AGC signal.

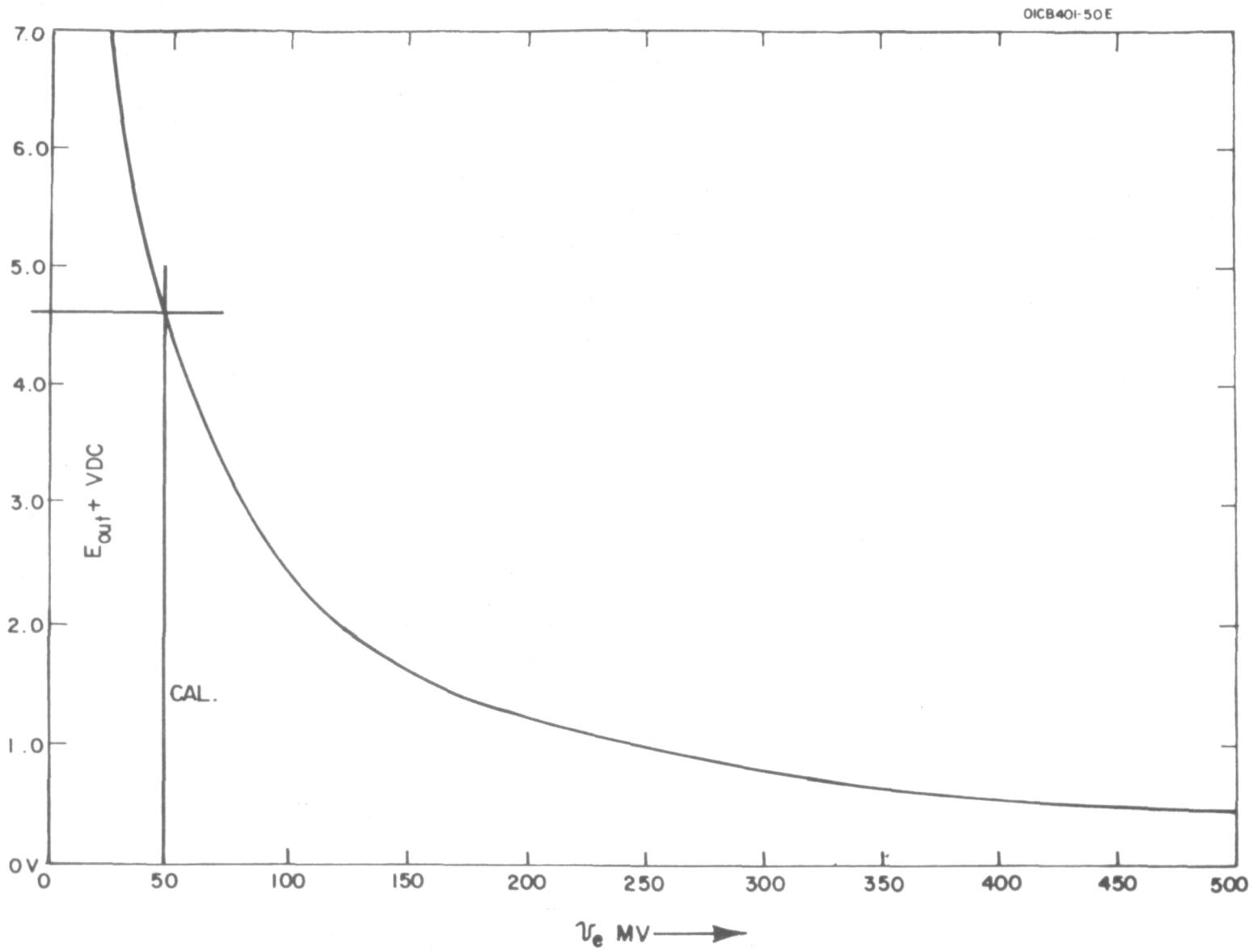

Figure 31. Modulation output versus electron energy (volts).

Page intentionally left blank

REFERENCES

1. Druyvesteyn, M. J., "Der Niedervoltbogen," Z. Phys. 64, 781-798 (1930).

2. Sloane, R. H. and MacGregor, E. I. R., "An Alternating Current Method for Collector Analylis of Discharge-Tubes," Phil. Mag. 18, 193-207 (1934).

3. Malyshev, G. M. and Federov, V. L., "Use of a Narrow-Band Amplifier in Oscillographic Investigation of the Electron Velocity Distribution Functions in an Electrical Discharge," Dokl. Acad. Nauk SSSR 92, 269-271 (1953).

4. Boyd, R. L. F. and Twiddy, N. D., "Electron Energy Distributions in Plasmas. I," Proc. Roy. Soc. 250, 53-69 (1959).

5. Branner, G. R., Friar, E. M. and Medicus, G., "Automatic Plotting Device for the Second Derivative of Langmuir Probe Curves," Rev. Sci. Inst. 34, 231-237 (1963).

6. Boyd, R. L. F. and Willmore, A. P., "A Method of Studying the Energy Distributions of Ionospheric Ions and Electrons," Space Research 3, pp. 1168-1173 (ed. Preister), North-Holland Publishing Co., Amsterdam (1963).

7. Bowen, P. J., Boyd, R. L. F., Henderson, C. L. and Willmore, A. P., "Measurement of Electron Temperature and Concentration from a Spacecraft," Proc. Roy. Soc. 281A, 514-525 (1964).